SARS-CoV-2 papain-like protease inhibits ISGylation of the viral nucleocapsid protein to evade host anti-viral immunity

Rhamadianti, Aulia Fitri ; Abe, Takayuki ; Tanaka, Tomohisa ; Ono, Chikako ; Katayama, Hisashi ; Makino, Yoshiteru ; Deng, Lin ; Matsui,…

(Citation)
Journal of Virology,98(9):e00855-24

(Issue Date)
2024-09-17

(Resource Type)
journal article

(Version)
Version of Record

Journal of Virology

Editor's Pick | Virology | Full-Length Text

SARS-CoV-2 papain-like protease inhibits ISGylation of the viral nucleocapsid protein to evade host anti-viral immunity

Aulia Fitri Rhamadianti,[1,2] Takayuki Abe,[1,3] Tomohisa Tanaka,[4,5] Chikako Ono,[6] Hisashi Katayama,[1] Yoshiteru Makino,[7,8] Lin Deng,[1] Chieko Matsui,[1] Kohji Moriishi,[4,5] Fumi Shima,[7] Yoshiharu Matsuura,[6,9] Ikuo Shoji[1]

AUTHOR AFFILIATIONS See affiliation list on p. 24.

ABSTRACT A severe acute respiratory syndrome coronavirus 2 (SARS-CoV-2) infection causes mild-to-severe respiratory symptoms, including acute respiratory distress. Despite remarkable efforts to investigate the virological and pathological impacts of SARS-CoV-2, many of the characteristics of SARS-CoV-2 infection still remain unknown. The interferon-inducible ubiquitin-like protein ISG15 is covalently conjugated to several viral proteins to suppress their functions. It was reported that SARS-CoV-2 utilizes its papain-like protease (PLpro) to impede ISG15 conjugation, ISGylation. However, the role of ISGylation in SARS-CoV-2 infection remains unclear. We aimed to elucidate the role of ISGylation in SARS-CoV-2 replication. We observed that the SARS-CoV-2 nucleocapsid protein is a target protein for the HERC5 E3 ligase-mediated ISGylation in cultured cells. Site-directed mutagenesis reveals that the residue K374 within the C-terminal spacer B-N3 (SB/N3) domain is required for nucleocapsid-ISGylation, alongside conserved lysine residue in MERS-CoV (K372) and SARS-CoV (K375). We also observed that the nucleocapsid-ISGylation results in the disruption of nucleocapsid oligomerization, thereby inhibiting viral replication. Knockdown of ISG15 mRNA enhanced SARS-CoV-2 replication in the SARS-CoV-2 reporter replicon cells, while exogenous expression of ISGylation components partially hampered SARS-CoV-2 replication. Taken together, these results suggest that SARS-CoV-2 PLpro inhibits ISGylation of the nucleocapsid protein to promote viral replication by evading ISGylation-mediated disruption of the nucleocapsid oligomerization.

IMPORTANCE ISG15 is an interferon-inducible ubiquitin-like protein that is covalently conjugated to the viral protein via specific Lys residues and suppresses viral functions and viral propagation in many viruses. However, the role of ISGylation in SARS-CoV-2 infection remains largely unclear. Here, we demonstrated that the SARS-CoV-2 nucleocapsid protein is a target protein for the HERC5 E3 ligase-mediated ISGylation. We also found that the residue K374 within the C-terminal spacer B-N3 (SB/N3) domain is required for nucleocapsid-ISGylation. We obtained evidence suggesting that nucleocapsid-ISGylation results in the disruption of nucleocapsid-oligomerization, thereby suppressing SARS-CoV-2 replication. We discovered that SARS-CoV-2 papain-like protease inhibits ISG15 conjugation of nucleocapsid protein via its de-conjugating enzyme activity. The present study may contribute to gaining new insight into the roles of ISGylation-mediated anti-viral function in SARS-CoV-2 infection and may lead to the development of more potent and selective inhibitors targeted to SARS-CoV-2 nucleocapsid protein.

KEYWORDS SARS-CoV-2, papain-like protease, nucleocapsid, ISG15, anti-viral activity

In December 2019, the novel coronavirus (CoV), also known as severe acute respiratory syndrome coronavirus 2 (SARS-CoV-2), was first reported in Wuhan, China. SARS-CoV-2

Editor Mark T. Heise, University of North Carolina at Chapel Hill, Chapel Hill, North Carolina, USA

Address correspondence to Ikuo Shoji, ishoji@med.kobe-u.ac.jp.

The authors declare no conflict of interest.

See the funding table on p. 25.

Received 15 May 2024
Accepted 29 June 2024
Published 9 August 2024

quickly spread all around the world. In March 2020, the World Health Organization declared a global pandemic of coronavirus disease 19 (COVID-19), which is caused by SARS-CoV-2. SARS-CoV-2 infection causes mild-to-severe respiratory symptoms, including fever, dry cough, breathing difficulties, and acute respiratory distress (1). The mRNA vaccine to produce the viral spike (S) protein induces a robust immune response against SARS-CoV-2, although the molecular mode of action and the possible adverse effects remain to be elucidated (2). Several anti-viral drugs, including favipiravir, remdesivir, molnupiravir, and viral protease inhibitors, have been developed for the treatment of COVID-19 (3, 4).

SARS-CoV-2 belongs to an enveloped beta-coronavirus genus of the family *Coronaviridae*. The viral genome possesses a positive-sense, single-stranded RNA that encodes 29 kb, consisting of 16 non-structural proteins (nsp1-16), 4 structural proteins [spike, nucleocapsid (also referred to as ORF9), envelope, and membrane proteins], and 7 accessory proteins (ORF3a, ORF3b, ORF6, ORF7a, ORF7b, ORF8, and ORF10) (5). The non-structural proteins form a replicase-transcriptase complex. The structural proteins form the mature virion. The accessory proteins manipulate the host response to facilitate viral replication and pathogenesis. SARS-CoV-2 papain-like protease (PLpro), encoded within nsp3, is required not only for processing the viral polyproteins but also for inhibiting ubiquitin and ubiquitin-like protein modifications (5–7). Despite remarkable efforts to investigate the virological and pathological impacts of SARS-CoV-2, many of the characteristics of SARS-CoV-2 still remain unknown (8).

The SARS-CoV-2 nucleocapsid protein contains 419 amino acids and consists of five domains: the N-terminal tail region (residues 1–50, termed N1a), the N-terminal RNA-binding domain (residues 51–174, termed NTD/N1b), the serine/arginine-rich region (residues 175–247, termed N2a), the C-terminal dimerization domain (residues 248–364, termed CTD/N2b), and the intrinsically disordered regions [residues 365–419, termed spacer B/N3 (SB/N3)] (9). Both the N-terminal domain (NTD) and the C-terminal domain (CTD) participate in the binding and packaging of the viral RNA genome into the virion (10–12). The C-terminal SB/N3 domain has been implicated in the involvement of CTD-mediated nucleocapsid oligomerization (9). Several studies have reported the crystal structure of the NTD and the CTD, while the detailed structural characterization and function of the SB/N3 domain have not been clarified yet (13). Indeed, the SARS-CoV-2 nucleocapsid protein was reported to antagonize the JAK-STAT-mediated interferon (IFN) signaling pathway and IFN-induced stress granule formation (14–16).

The innate immune-mediated IFN signaling pathway is activated by viral and bacterial infection to produce hundreds of IFN-stimulated genes (ISGs) (17). ISG15, which is one of the ubiquitin-like proteins, is covalently conjugated to the target protein via specific lysine (Lys) residues by three intracellular enzymes, i.e., E1 activating enzyme (UBE1L), E2 conjugating enzyme (UbcH8), and E3 ligase (HERC5) (17). This process is called ISGylation and is a posttranslational protein modification that is similar to ubiquitylation (18). The covalently conjugated ISG15 is removed from ISGylated proteins by USP18 (also referred to as UBP43), an ISG15-deconjugating enzyme (19). The ISG15/ISGylation has been suggested to function as an anti-viral factor against several RNA and DNA viruses (18, 20, 21). However, we previously reported that the ISG15/ISGylation possesses a proviral function that promotes HCV and HBV infection (22, 23).

In the present study, we aimed to elucidate the role of ISGylation in SARS-CoV-2 replication. We demonstrate that the SARS-CoV-2 nucleocapsid protein is a target protein for the HERC5 E3 ligase-mediated ISGylation in cultured cells and that the residue K374 within the SB/N3 domain is required for nucleocapsid-ISGylation. We also demonstrate that nucleocapsid-ISGylation results in the disruption of nucleocapsid oligomerization, thereby inhibiting viral replication. Finally, we demonstrate that SARS-CoV-2 PLpro inhibits ISGylation of the nucleocapsid protein to evade the ISGylation-mediated anti-viral activity.

RESULTS

SARS-CoV-2 nucleocapsid protein is a target protein for ISGylation

To identify a target protein for ISGylation in the different SARS-CoV-2 proteins, we co-transfected 293T cells with plasmids carrying E1 (UBE1L), E2 (UbcH8), E3 (HERC5), and FLAG-ISG15 together with a series of viral proteins, i.e., non-structural proteins (nsp1 to 16, except for nsp3 and nsp11) (Fig. 1A through N), structural proteins (membrane, spike, envelope, or nucleocapsid proteins) (Fig. 1O through Q; Fig. 2), and ORF proteins (3a, 6, 7a, 7b, 8, and 10, except for 3b) (Fig. 1R through W). We used epitope-tagged (N-terminal HA-tag, C-terminal Myc-His_6-tag, or N-terminal EGFP-tag) viral proteins. Then, we analyzed ISGylation of the viral proteins by immunoblotting with detection with anti-HA, anti-Myc, or anti-EGFP antibodies, respectively. We could not test nsp3, nsp11, and ORF3b because the expression levels of these proteins were too low.

The immunoprecipitation analysis coupled with immunoblotting revealed that no other examined viral proteins except nucleocapsid showed the ISGylated forms and precipitation with FLAG-ISG15 (Fig. 1) and that only the nucleocapsid protein was precipitated with FLAG-ISG15, and the ISGylated forms of the nucleocapsid protein were clearly detected (Fig. 2A, first and second panels, lane 3, asterisks). In the immunoblot analysis with anti-FLAG antibody, FLAG-ISG15 and its conjugates were detected only in the cells co-expressed with E1/E2/E3 components (Fig. 2A, bottom panel, lane 3). These results suggest that the nucleocapsid protein specifically accepts ISGylation among all the SARS-CoV-2 proteins tested.

Next, to verify the specificity of nucleocapsid-ISGylation, we performed the ISGylation assay using a conjugation-defective ISG15 mutant that possesses the Gly-Gly to Ala-Ala substitution within the C-terminal LRLRGG motif sequence (referred to as FLAG-ISG15-AA). The expression of FLAG-ISG15-AA resulted in the loss of interaction between FLAG-ISG15-AA and nucleocapsid protein as well as nucleocapsid-ISGylation (Fig. 2A, first and second panels: compare lane 3 with lane 4). These results suggest that the SARS-CoV-2 nucleocapsid protein is a specific target for ISGylation.

Furthermore, to confirm whether these slowly migrating forms of the nucleocapsid protein are indeed ISG15-conjugated nucleocapsid proteins, we performed the immunoprecipitation analysis with anti-Myc antibody (9E10) following the detection with anti-nucleocapsid antibody (HL448) or anti-ISG15 antibody (F-9), respectively. As shown in Fig. 2B and C, the slowly migrating forms of the nucleocapsid protein were also detected with anti-nucleocapsid antibody and anti-ISG15 antibody, indicating that the slowly migrating forms of the nucleocapsid protein were indeed the ISG15-conjugated (ISGylated) nucleocapsid proteins.

To determine whether the nucleocapsid proteins produced from SARS-CoV-2 reporter replicon cells (VeroE6/Rep3) are ISGylated, we performed the ISGylation assay using VeroE6/Rep3 cells. The immunoblot analysis of the VeroE6/Rep3 cell lysates showed that ISGylated nucleocapsid proteins were hardly detected (Fig. 2D, third panel, lane 2). However, the immunoprecipitation coupled with immunoblot analysis revealed that nucleocapsid proteins produced from the VeroE6/Rep3 cells were indeed ISGylated (Fig. 2D, top panel, lane 2).

To further examine the differences in nucleocapsid-ISGylation among other coronaviruses, we performed the ISGylation assay of the nucleocapsid proteins from SARS-CoV (WH20 strain, accession no. NP828858.1) and MERS-CoV (EMC/2012 strain, accession no. AFS88943.1). The alignment of the amino acid sequences on the nucleocapsid proteins revealed that SARS-CoV-2 and SARS-CoV or SARS-CoV-2 and MERS-CoV nucleocapsid proteins share 72.8% and 52.6% amino acid sequence similarities, respectively (Fig. 3). We observed the ISGylated forms of nucleocapsid proteins from SARS-CoV and MERS-CoV in their co-expressed cells (Fig. 4, first panel, lanes 3 and 6). These results suggest that the nucleocapsid proteins from MERS-CoV, SARS-CoV, and SARS-CoV-2 are target proteins for ISGylation.

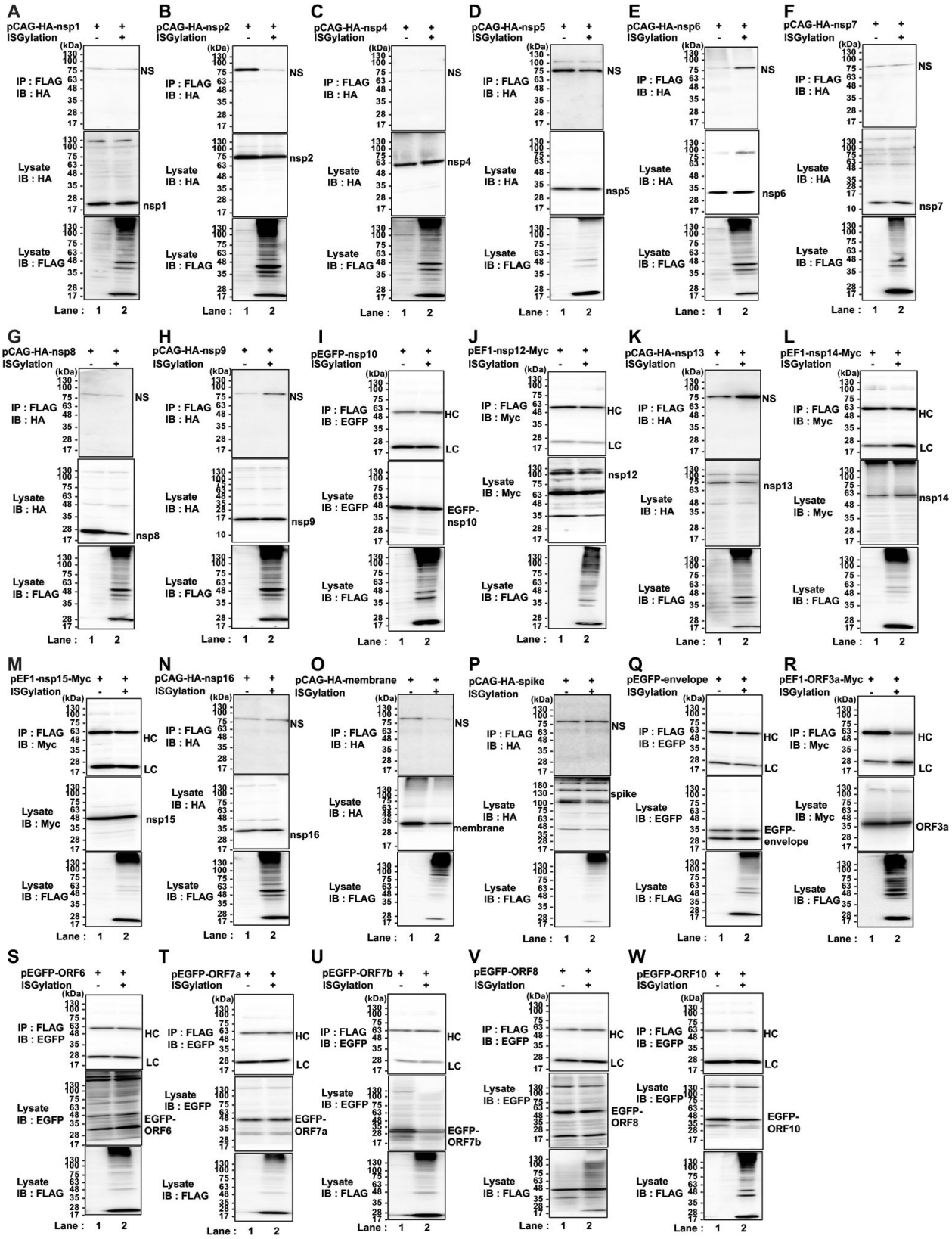

FIG 1 ISGylation assay of SARS-CoV-2 proteins. HEK293T cells were transfected with the expression plasmid encoding N-terminal HA, C-terminal Myc-His_6, or N-terminal EGFP-fused non-structural proteins (nsp1 to 16, except for nsp3 and nsp11) (A–N), structural proteins (membrane, spike, or envelope) (O–Q), and ORF proteins (3a, 6, 7a, 7b, 8, and 10, except for 3b) (R–W) and FLAG-ISG15 together with E1 (UBE1L), E2 (UbcH8), and E3 (HERC5), followed by immunoprecipitation

(Continued on next page)

FIG 1 (Continued)

with anti-FLAG mouse monoclonal antibody (mAb (M2) and detection with anti-HA, anti-Myc, or EGFP antibodies, respectively. IP, immunoprecipitation; IB, immunoblotting; NS, non-specific band; LC, light chain; HC, heavy chain. Input samples (indicated as lysate) were detected with anti-FLAG mouse mAb (M2). The immunoblots are representative of three independent experiments.

HERC5 is a specific E3 ligase for ISGylation of the SARS-CoV-2 nucleocapsid protein

Next, to investigate the specificity of E3 ligases for nucleocapsid-ISGylation, we co-expressed SARS-CoV-2 nucleocapsid-Myc-His_6 and one of three different HA-tagged E3 ligases, i.e., HA-HERC5 (a), HA-TRIM25 (b), or HA-HHARI (c), together with FLAG-ISG15, E1 (UBE1L), and E2 (UbcH8) in 293T cells, followed by immunoprecipitation with anti-FLAG antibody and detection with anti-nucleocapsid antibody (HL448). The immunoblot analysis revealed that HERC5 protein, but neither TRIM25 nor HHARI, promoted nucleocapsid-ISGylation (Fig. 5A, first and second panels, lanes 3–5). The immunoblot analysis with anti-FLAG antibody revealed that nucleocapsid-ISGylation was detected only in the cells expressed with HA-HERC5 protein (Fig. 5A, bottom panel, lane 3). These results suggest that HERC5 is a specific E3 ligase for nucleocapsid-ISGylation.

Next, to verify that HERC5 protein ligase activity is involved in nucleocapsid-ISGylation, we performed the ISGylation assay of the SARS-CoV-2 nucleocapsid protein using the catalytically inactive mutant HA-HERC5 (C994A). HA-HERC5 WT induced nucleocapsid-ISGylation, whereas HA-HERC5 (C994A) mutant resulted in a loss of nucleocapsid-ISGylation (Fig. 5B, first and second panels: compare lane 3 with lane 4). These results suggest that HERC5 protein ligase activity is required for nucleocapsid-ISGylation.

The residues K143 and K347 are acceptor lysines for ISGylation on SARS-CoV-2 nucleocapsid protein

The SARS-CoV-2 nucleocapsid protein is composed of the N1a domain, the NTD, the N2a domain, the CTD, and the SB/N3 domain. The SARS-CoV-2 nucleocapsid protein contains 31 Lys (K) residues within these five domains described above (Fig. 6A and 3). The N1a, NTD, N2a, CTD, and SB/N3 domains contain 1, 7, 2, 12, and 9 Lys residues, respectively. At first, to map the ISGylation sites on the nucleocapsid protein of SARS-CoV-2, we performed the ISGylation assay using the deletion mutants that we designated as the NTD and the N2a-CTD nucleocapsid deletion mutants (Fig. 6A). Immunoblot analysis revealed that the expression of either the NTD or the N2a-CTD nucleocapsid deletion mutants resulted in two forms of nucleocapsid-ISGylation, suggesting the existence of Lys residues for ISGylation within the NTD and N2a-CTD (Fig. 6B, first panel, lanes 4 and 6, asterisks).

To determine the Lys residue responsible for nucleocapsid-ISGylation within the NTD and N2a-CTD, we then constructed a series of nucleocapsid mutants containing a point mutation of Arg (R) at a corresponding Lys (K) within the NTD or the N2a-CTD. Using the K/R mutants of the nucleocapsid, we observed that the levels of nucleocapsid-ISGylation were reduced compared to those of the nucleocapsid WT-Myc-His_6, only when the nucleocapsid K143R-Myc-His_6 and nucleocapsid K347R-Myc-His_6 were expressed (Fig. 6C, first panel: compare lane 2 with lanes 4 and 5). The full-length nucleocapsid protein possessing a K38R mutation exhibited ISGylation comparable to that of the WT nucleocapsid, suggesting that the K38 residue is not involved in the nucleocapsid-ISGylation (Fig. 6C, first panel: compare lanes 2 and 3). On the other hand, the nucleocapsid protein with all Lys residues mutated to Arg residues (referred to as nucleocapsid K-Null-Myc-His_6) did not show nucleocapsid-ISGylation (Fig. 6C, first panel, lane 6). The levels of nucleocapsid-ISGylation were unchanged compared to the nucleocapsid WT-Myc-His_6, when other K/R mutants of the nucleocapsid in the NTD or N2a-CTD were expressed (Fig. 7A and B).

We further analyzed the location of residues K143 in the NTD and K347 in the CTD on the 3D structure of the SARS-CoV-2 nucleocapsid with the program UCSF Chimera (Fig.

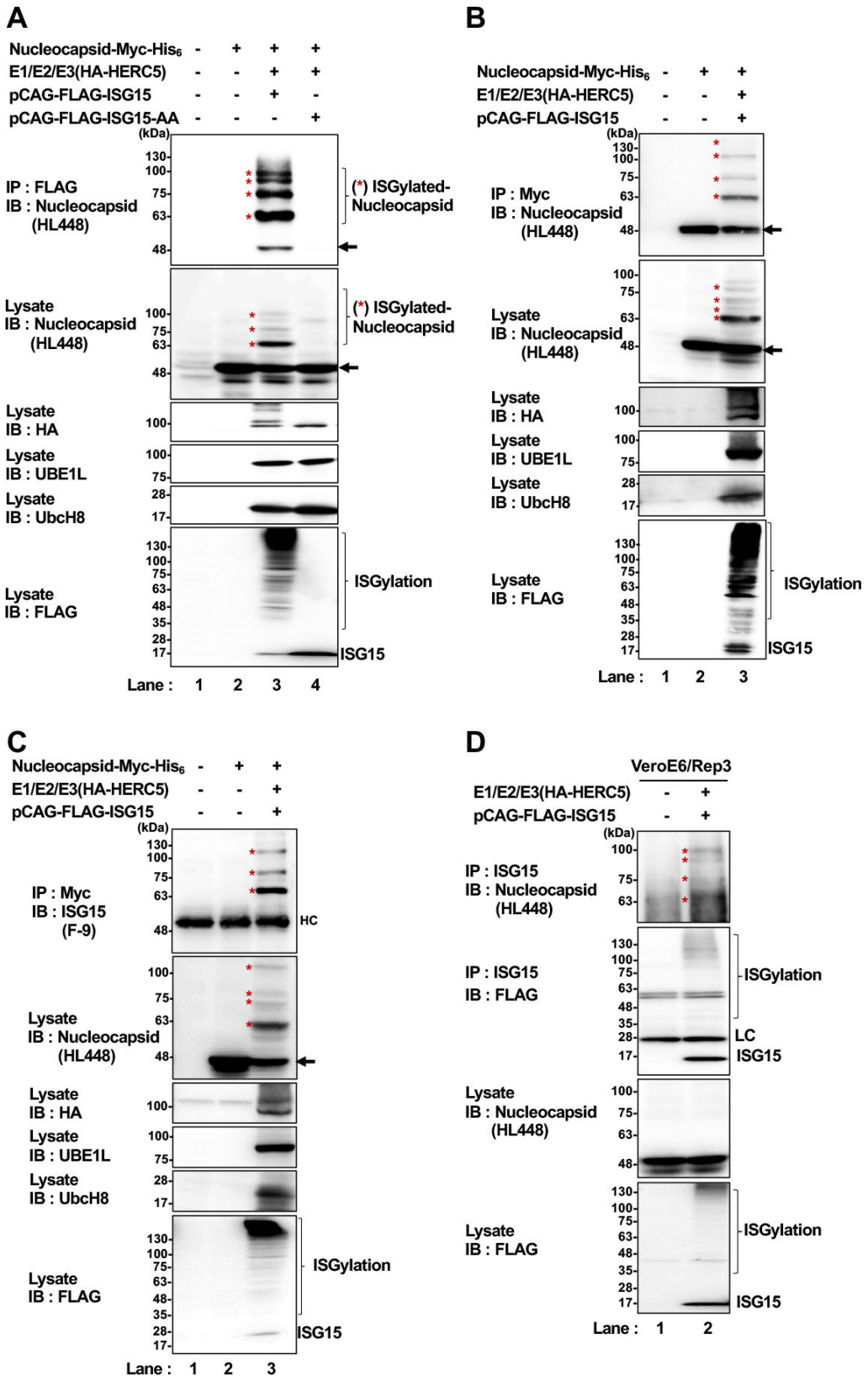

FIG 2 The SARS-CoV-2 nucleocapsid is a target protein for ISGylation, and HERC5 is a specific E3 ligase for nucleocapsid-ISGylation. (A) The expression plasmid encoding pEF1-nucleocapsid-Myc-His$_6$ from SARS-CoV-2 (WK-512) was co-expressed with either the pCAG-FLAG-ISG15 or FLAG-ISG15 mutant (pCAG-FLAG-ISG15-AA) together with pCAG-UBE1L (E1), pCAG-UbcH8

(Continued on next page)

FIG 2 (Continued)

(E2), and pCAG-HA-HERC5 (E3 ligase) in 293T cells, followed by immunoprecipitation with anti-FLAG mouse mAb (M2) and detection with anti-nucleocapsid rabbit mAb (HL448). (B and C) The expression plasmid nucleocapsid-Myc-His_6 from SARS-CoV-2 (WK-512) was co-expressed with pCAG-FLAG-ISG15 together with E1, E2, and E3 ligase in 293T cells, followed by immunoprecipitation with anti-Myc mouse mAb (9E10) and detection with anti-nucleocapsid rabbit mAb (HL448) (B) or anti-ISG15 mouse mAb (F-9) (C), respectively. Input samples (indicated as lysate) were detected with anti-nucleocapsid rabbit mAb (HL448), anti-UBE1L rabbit mAb, anti-UbcH8 mouse mAb, anti-HA rabbit polyclonal antibody (pAb), or anti-FLAG mouse mAb (M2) as indicated. (D) SARS-CoV-2 reporter replicon cells (VeroE6/Rep3) were transfected with the expression plasmid pCAG-FLAG-ISG15 together with pCAG-UBE1L (E1), pCAG-UbcH8 (E2), and pCAG-HA-HERC5 (E3 ligase). Cells were harvested, and cell lysates were immunoprecipitated with anti-ISG15 mouse mAb (F-9) followed by detection with anti-nucleocapsid rabbit mAb (HL448) or anti-FLAG-mouse mAb (M2). Input samples (indicated as lysate) were detected with anti-nucleocapsid rabbit mAb (HL448) and anti-FLAG-mouse mAb (M2). Asterisk (*) indicates the ISG15-conjugated nucleocapsid proteins (ISGylated-nucleocapsid). The arrow indicates an authentic size of nucleocapsid-Myc-His_6. The immunoblots are representative of three independent experiments.

8A and B). Residue K143 is located near residue R149, which plays a key role in capturing viral RNA. The residue K347 is located in the longest alpha-5 helix, which interacts with the beta-1 strand. These results suggest that the residues K143 in the NTD and K347 in the CTD are accessible by E3 ligase for ISGylation and acceptor lysines for ISGylation on SARS-CoV-2 nucleocapsid protein.

The residue K374 in the SB/N3 domain of the SARS-CoV-2 nucleocapsid protein is a major acceptor lysine for ISGylation

Next, to identify the acceptor lysine residue for ISGylation in the SB/N3 domain, we constructed nine different mutants in which Lys (K) was replaced with Arg (R) in the SB/N3 domain on the nucleocapsid protein (Fig. 9A). Immunoblot analysis revealed that the levels of nucleocapsid-ISGylation were dramatically reduced when the nucleocapsid K374R-Myc-His_6 was expressed (Fig. 9B, first and second panels, lane 7). These results suggest that the residue K374 in SB/N3 is a major acceptor lysine for ISGylation.

The alignment of the amino acid sequences of the SB/N3 domain among MERS-CoV, SARS-CoV, and SARS-CoV-2 revealed that both the residue K372 from MERS-CoV and the residue K375 from SARS-CoV correspond to the residue K374 from SARS-CoV-2 (Fig. 3). To verify that these conserved Lys (K) residues from SARS-CoV and MERS-CoV are responsible for the nucleocapsid-ISGylation, we performed the ISGylation assay using MERS-CoV nucleocapsid mutant K372R and SARS-CoV nucleocapsid mutant K375R. Immunoblot analysis revealed that nucleocapsid-ISGylation was markedly reduced compared to the nucleocapsid-Myc-His_6 WT, when either the MERS-CoV nucleocapsid K372R-Myc-His_6 or SARS-CoV nucleocapsid K375R-Myc-His_6 was expressed (Fig. 9C). These results suggest that the major Lys (K) residues responsible for nucleocapsid-ISGylation are conserved among MERS-CoV, SARS-CoV, and SARS-CoV-2.

SARS-CoV-2 PLpro de-ISGylates the nucleocapsid protein

Based on the fact that SARS-CoV-2 PLpro acts as a de-conjugating enzyme for ISGylation and ubiquitination, we hypothesized that PLpro may cleave ISG15 on the ISGylated nucleocapsid protein. To address this hypothesis, we co-expressed SARS-CoV-2 nucleocapsid-Myc-His_6 and FLAG-PLpro together with ISGylation machinery components, including untagged-ISG15, E1 (UBE1L), E2 (UbcH8), and E3 (HA-HERC5) in 293T cells, followed by immunoprecipitation with anti-ISG15 antibody and detection with anti-nucleocapsid antibody (HL448). The expression of PLpro, but not its catalytically inactive mutant PLpro (C111S), exhibited the marked reduction of nucleocapsid-ISGylation and the intracellular ISGylation (Fig. 10A, first, second, and seventh panels, lanes 3–5). Furthermore, treatment with a specific PLpro inhibitor (referred to as GRL-0617) resulted in the recovery of both the nucleocapsid-ISGylation and the intracellular

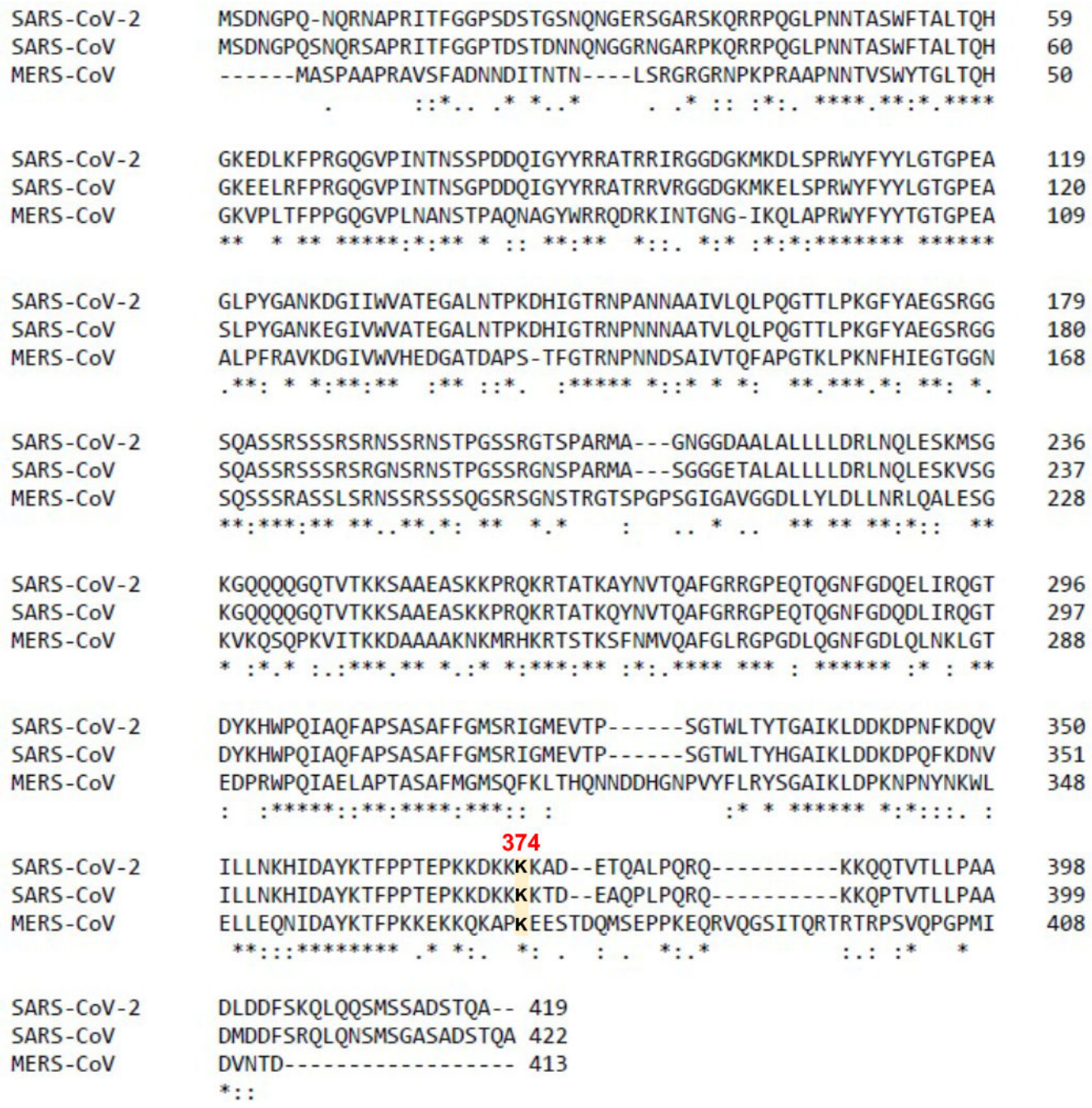

FIG 3 Sequence alignment of the nucleocapsid proteins from MERS-CoV, SARS-CoV, and SARS-CoV-2. Amino acid sequence alignment of the MERS-CoV (EMC/2012 strain) and SARS-CoV (WH20 strain) to SARS-CoV-2 (WK-512 strain).

ISGylation (Fig. 10B, first, second, and seventh panels, lanes 2–6). These results suggest that SARS-CoV-2 PLpro de-ISGylates the nucleocapsid protein.

To further elucidate the role of PLpro in de-ISGylation of the nucleocapsid protein, we co-expressed nucleocapsid-Myc-His_6 and V5-tagged PLpro from SARS-CoV or MERS-CoV together with ISGylation components in 293T cells. The results showed that PLpro from SARS-CoV or MERS-CoV efficiently cleaves ISG15 from their ISGylated nucleocapsid proteins (Fig. 11, first panel, lanes 2–3 or lanes 5–6). These results suggest that PLpro from SARS-CoV or MERS-CoV has the ability to de-ISGylate the nucleocapsid proteins.

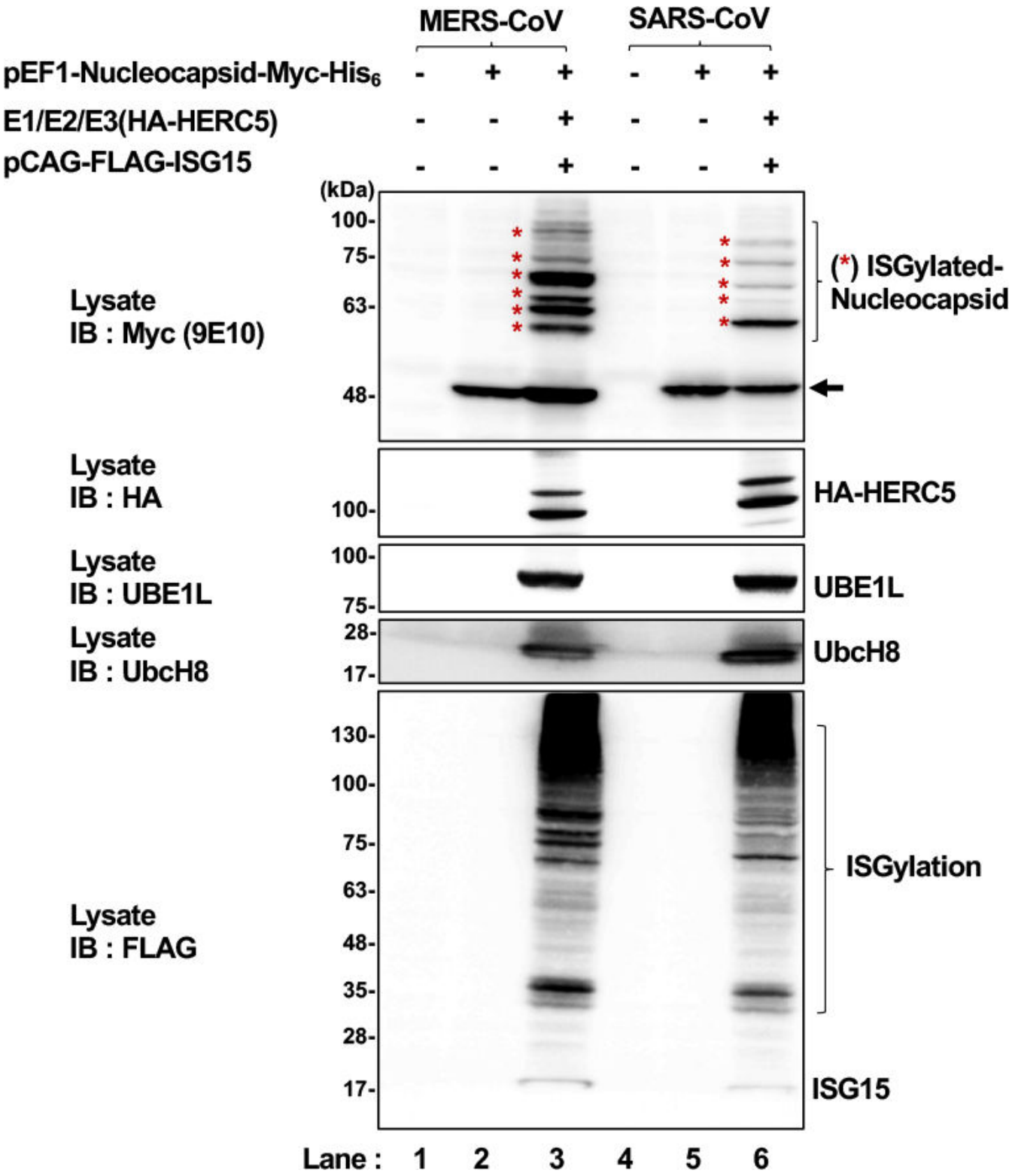

FIG 4 The nucleocapsid protein is a target for ISGylation in the different *betacoronaviruses*. The expression plasmid encoding nucleocapsid-Myc-His_6 (pEF1-nucleocapsid-Myc-His_6) from SARS-CoV (WH20 strain) or MERS-CoV (EMC/2012 strain) was co-expressed with pCAG-FLAG-ISG15 together with pCAG-UBE1L (E1), pCAG-UbcH8 (E2), and pCAG-HA-HERC5 in 293T cells, followed by the detection with anti-Myc mouse mAb (9E10). Input samples (indicated as lysate) were detected with anti-UBE1L rabbit mAb, anti-UbcH8 mouse mAb, anti-HA rabbit pAb, or anti-FLAG mouse mAb (M2) as indicated. Asterisk (*) indicates the ISG15-conjugated nucleocapsid proteins (ISGylated-nucleocapsid). The arrow indicates an authentic size of nucleocapsid-Myc-His_6. The immunoblots are representative of three independent experiments.

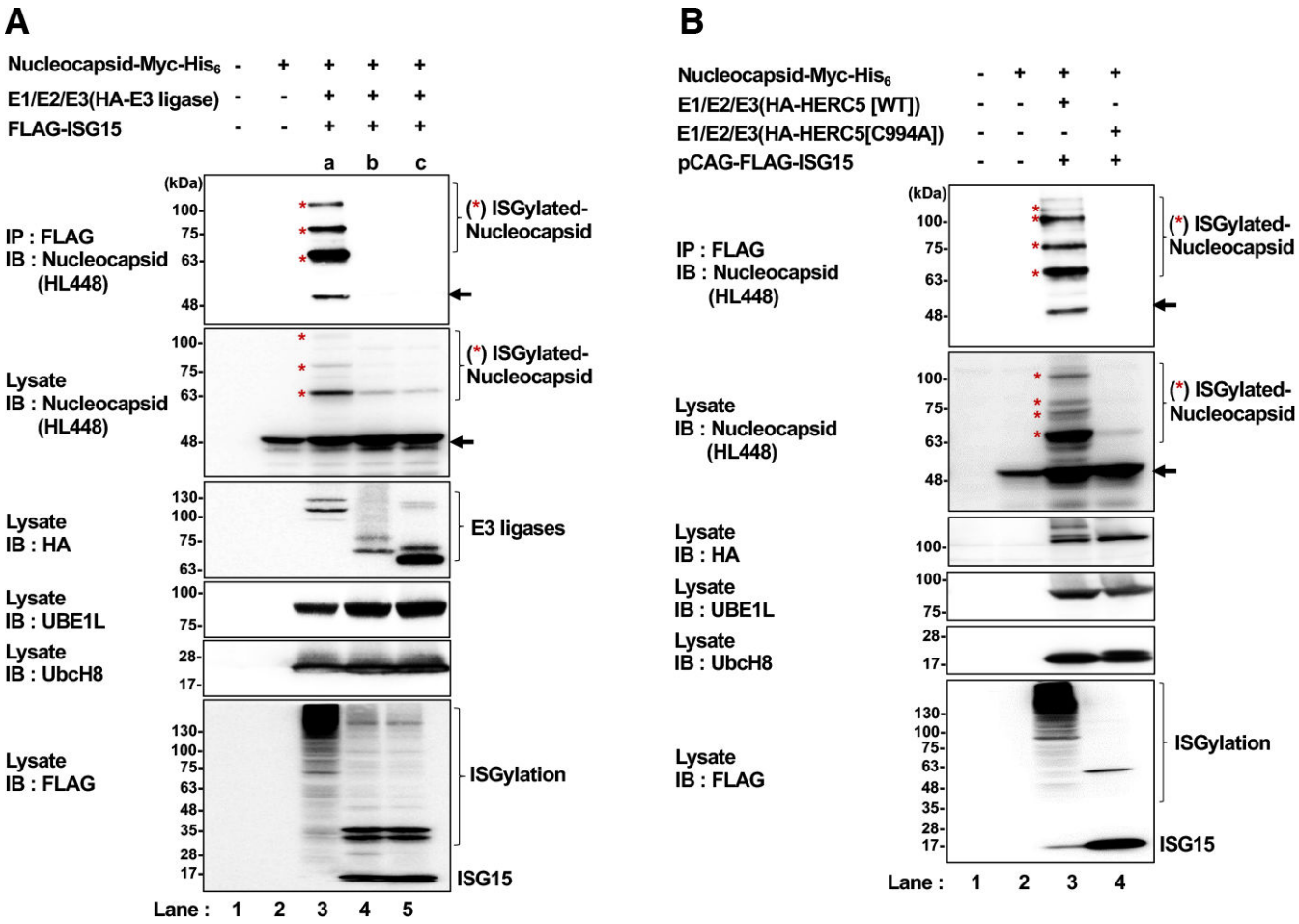

FIG 5 HERC5 is a specific E3 ligase for ISGylation of the SARS-CoV-2 nucleocapsid protein. (A) The expression plasmid encoding nucleocapsid-Myc-His_6 (pEF1-nucleocapsid-Myc-His_6) from SARS-CoV-2 (WK-512) was co-expressed with pCAG-FLAG-ISG15 and an HA-tagged E3 ligase, i.e., (a) pCAG-HA-HERC5, (b) pCAG-HA-TRIM25, or (c) pCAG-HA-HHARI together with pCAG-UBE1L (E1) and pCAG-UbcH8 (E2) in 293T cells, followed by immunoprecipitation with anti-FLAG mouse mAb (M2) and detection with anti-nucleocapsid rabbit mAb (HL448). (B) The expression plasmid encoding nucleocapsid-Myc-His_6 from SARS-CoV-2 (WK-512) was co-expressed with pCAG-FLAG-ISG15 together with E1, E2, and pCAG-HA-HERC5 [wild type (WT)] or the catalytically inactive mutant pCAG-HA-HERC5 C994A in 293T cells, followed by immunoprecipitation with anti-FLAG mouse mAb (M2) and detection with anti-nucleocapsid rabbit mAb (HL448). Input samples (indicated as lysate) were detected with anti-nucleocapsid rabbit mAb (HL448), anti-UBE1L rabbit mAb, anti-UbcH8 mouse mAb, anti-HA rabbit pAb, or anti-FLAG mouse mAb (M2) as indicated. Asterisk (*) indicates the ISG15-conjugated nucleocapsid proteins (ISGylated-nucleocapsid). The arrow indicates an authentic size of nucleocapsid-Myc-His_6. The immunoblots are representative of three independent experiments.

ISG15 induces anti-viral activity in the SARS-CoV-2 replication

To determine the role(s) of ISG15/ISGylation in SARS-CoV-2 replication, we performed small interfering (si)RNA-mediated knockdown of ISG15 mRNA in the SARS-CoV-2 reporter replicon cells derived from VeroE6 cells (VeroE6/Rep3). The SARS-CoV-2 reporter replicon cells possess replicon RNA with a gene encoding *Renilla* luciferase (R-luc) to monitor the level of viral replication. We then designed two different siRNAs targeted to the coding region of ISG15 derived from an African green monkey (agm) (Fig. 12A, referred to as siRNA Monkey (Mo)-ISG15 #1 and siRNA Mo-ISG15 #2).

The target sequence of siRNA Mo-ISG15 #2 is conserved between Mo-ISG15 and human ISG15, while siRNA#1 is specific for Mo-ISG15, containing a mismatch to human ISG15 (Fig. 12A). The knockdown efficiencies of endogenous Mo-ISG15 by siRNA#1 and siRNA#2 were approx. 80% and 90% in the VeroE6/Rep3 cells, respectively (Fig. 12B, middle panel, lanes 2 and 3; Fig. 12C, right panel). In particular, the knockdown of endogenous Mo-ISG15 by siRNA Mo-ISG15 #1 enhanced the expression of the viral

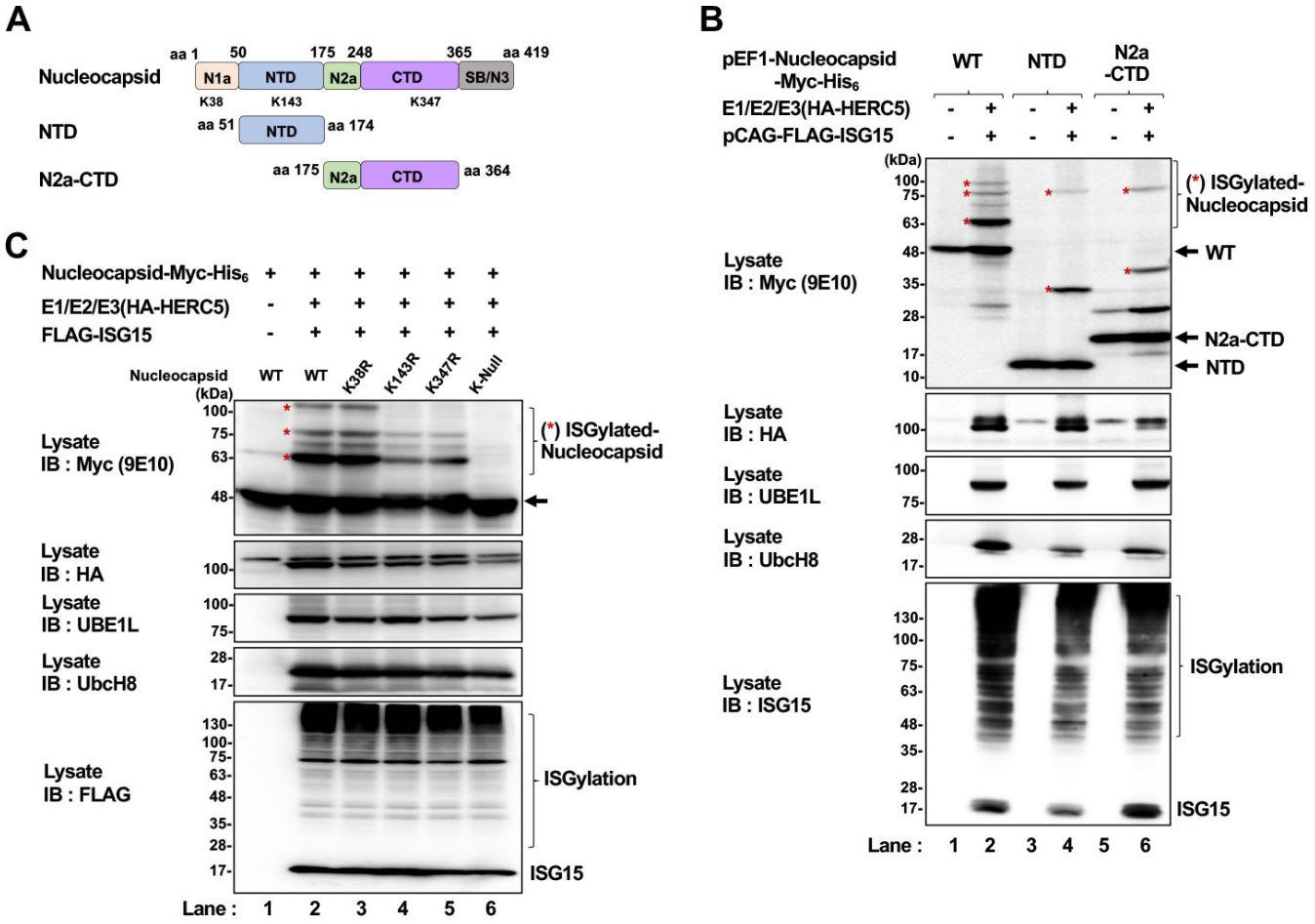

FIG 6 The residues K143 and K347 of SARS-CoV-2 nucleocapsid protein accept ISGylation. (A) Schematic diagram of the WT or deletion mutants of the nucleocapsid protein of SARS-CoV-2 (WK-512). The NTD covers from amino acid 51 to 174. The N2a-CTD covers from amino acid 175 to 364. (B) The expression plasmid encoding either nucleocapsid-Myc-His_6 from SARS-CoV-2 (WK-512) or nucleocapsid deletion mutants (NTD and N2a-CTD) was co-expressed with pCAG-FLAG-ISG15 together with E1, E2, and E3 ligase (HA-HERC5) in 293T cells, followed by detection with anti-Myc mouse mAb (9E10). Input samples (indicated as lysate) were detected with anti-Myc mouse mAb (9E10), anti-UBE1L rabbit mAb, anti-UbcH8 mouse mAb, anti-HA rabbit pAb, or anti-FLAG mouse mAb (M2) as indicated. Asterisks (*) indicate the ISG15-conjugated nucleocapsid proteins (ISGylated-nucleocapsid). (C) The expression plasmid encoding nucleocapsid-Myc-His_6 (pEF1-nucleocapsid-Myc-His_6) of SARS-CoV-2 (WK-512) or Lys mutants containing a point mutation of Lys to Arg at the corresponding Lys residues (K38R, K143R, and K347R) on the full-length nucleocapsid were co-expressed with pCAG-FLAG-ISG15 together with pCAG-UBE1L (E1), pCAG-UbcH8 (E2), and pCAG-HA-HERC5 (E3) in 293T cells, followed by detection with anti-Myc mouse mAb (9E10). Input lysates were detected with anti-UBE1L rabbit mAb, anti-UbcH8 mouse mAb, anti-HA rabbit pAb, or anti-FLAG mouse mAb (M2) as indicated. Asterisk (*) indicates the ISGylated nucleocapsid-Myc-His_6 proteins. The arrow indicates an authentic size of nucleocapsid-Myc-His_6, N2a-CTD, or NTD. The Western blots are representative of three independent experiments.

nucleocapsid protein, sub-genomic replicon RNA (sgRNA), and viral replication-mediated R-luc activity compared to those in VeroE6/Rep3 cells transfected with NC siRNA (Fig. 12B, top panel, lane 2; Fig. 12C, left panel; Fig. 12D). Next, in a gain-of-function experiment, we co-expressed ISGylation machinery components, including either FLAG-ISG15 or FLAG-ISG15-AA mutant, together with UBE1L (E1), UbcH8 (E2), or HERC5 (E3) in VeroE6/Rep3 cells. The overexpression of ISGylation machinery components including FLAG-ISG15, but not FLAG-ISG15-AA mutant, resulted in a marked reduction of viral replication-mediated R-luc activity and viral nucleocapsid protein in VeroE6/Rep3 cells (Fig. 12E and F, upper panel, lane 3). These results suggest that ISG15/ISGylation functions as anti-viral activity in the SARS-CoV-2 replicating cells.

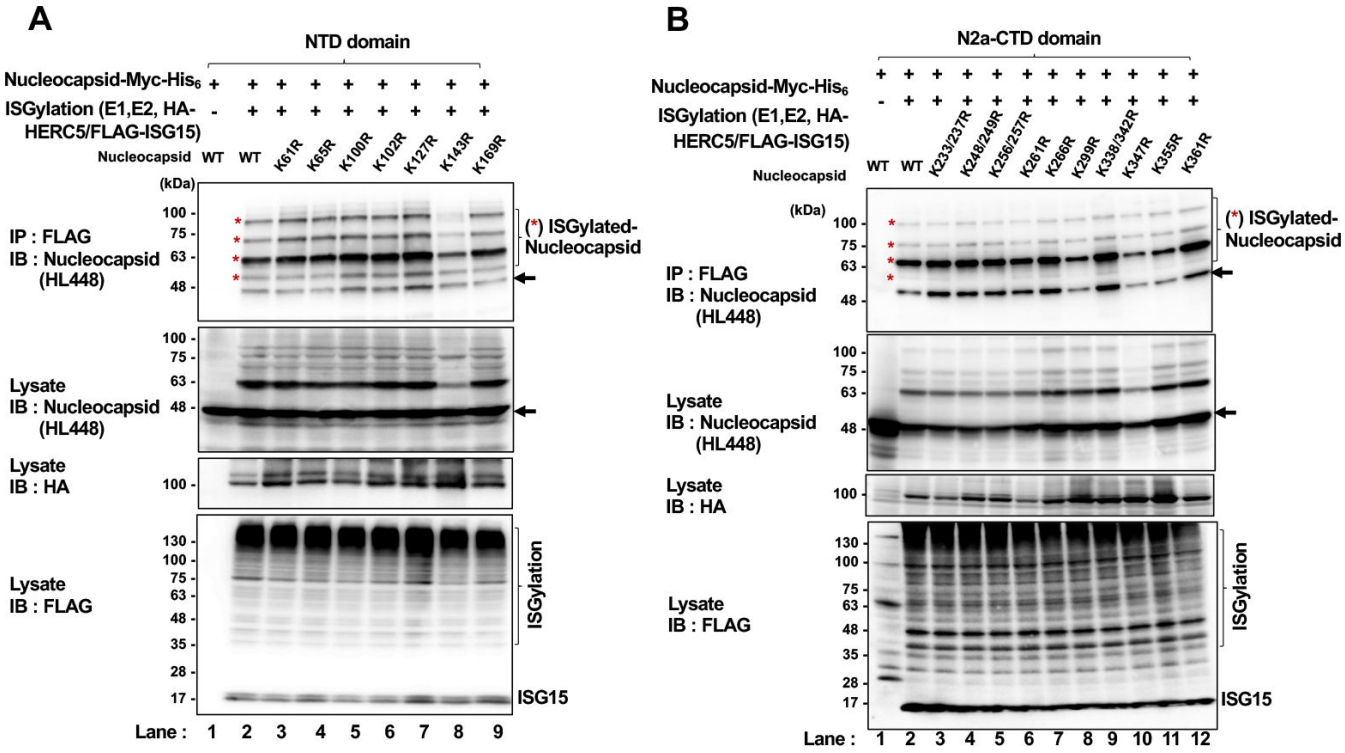

FIG 7 ISGylation assay of NTD and N2a-CTD of nucleocapsid. (A and B) The expression plasmid encoding nucleocapsid-Myc-His_6 (pEF1-nucleocapsid-Myc-His_6) from SARS-CoV-2 (WK-512) or nucleocapsid Lys (K) mutants containing a point mutation of Lys to Arg at the corresponding Lys residues in NTD (K61R, K65R, K100R, K102R, K127R, K143R, K169R) or N2a-CTD (K233/237R, K248/249R, K256/257R, K261R, K266R, K299R, K338/342R, K347R, K355R, and K361R) were co-expressed with pCAG-FLAG-ISG15 together with pCAG-UBE1L (E1), pCAG-UbcH8 (E2), and HA-tagged E3 ligase (pCAG-HA-HERC5) in 293T cells, followed by immunoprecipitation with anti-FLAG mouse mAb (M2) and detection with anti-nucleocapsid rabbit mAb (HL448). Input samples were detected with anti-nucleocapsid rabbit mAb (HL448), anti-HA rabbit pAb, or anti-FLAG mouse mAb (M2) as indicated. The arrow indicates an authentic size of nucleocapsid-Myc-His_6. The immunoblots are representative of three independent experiments.

ISGylation inhibits SARS-CoV-2 replication by disrupting viral nucleocapsid oligomerization

Finally, we investigated the role(s) of nucleocapsid-ISGylation in anti-viral activity in the SARS-CoV-2 replicating cells. We examined the effect of ISGylation on the oligomerization of the nucleocapsid protein in the 293T cells expressed with SARS-CoV-2 nucleocapsid-Myc-His_6. For this purpose, we performed native-polyacrylamide gel electrophoresis (PAGE) for the analysis of nucleocapsid-oligomerization. The native-PAGE of the WT nucleocapsid protein showed that nucleocapsid oligomerization was clearly detected (Fig. 13A, lane 1). We observed a marked decrease in the nucleocapsid-oligomer and nucleocapsid-dimer in the cells co-expressed with HA-HERC5 together with E1, E2, and FLAG-ISG15 (Fig. 13A, lane 2), compared to the nucleocapsid-oligomer in the cells expressed with HA-HERC5 (C994A) mutant together with E1, E2, and FLAG-ISG15, which was unchanged (Fig. 13A, lane 3). The detectable monomer nucleocapsid was very limited presumably because the authentic nucleocapsid was efficiently ISGylated when the wild-type ISGylation components were expressed (Fig. 13A, upper panel, lane 2). We also observed that knockdown of endogenous ISG15 enhanced nucleocapsid oligomerization in the 293T cells expressed with nucleocapsid-Myc-His_6 (Fig. 13B, lane 2) and in the VeroE6/Rep3 cells (Fig. 13C, lane 2). These results suggest that ISGylation inhibits nucleocapsid oligomerization, thereby suppressing viral replication.

To determine whether ISGylation at K374 in the SB/N3 domain of the nucleocapsid protein inhibits nucleocapsid-oligomerization, we assessed the impact of mutation at K374 in the SB/N3 domain on nucleocapsid-oligomerization. We observed that the

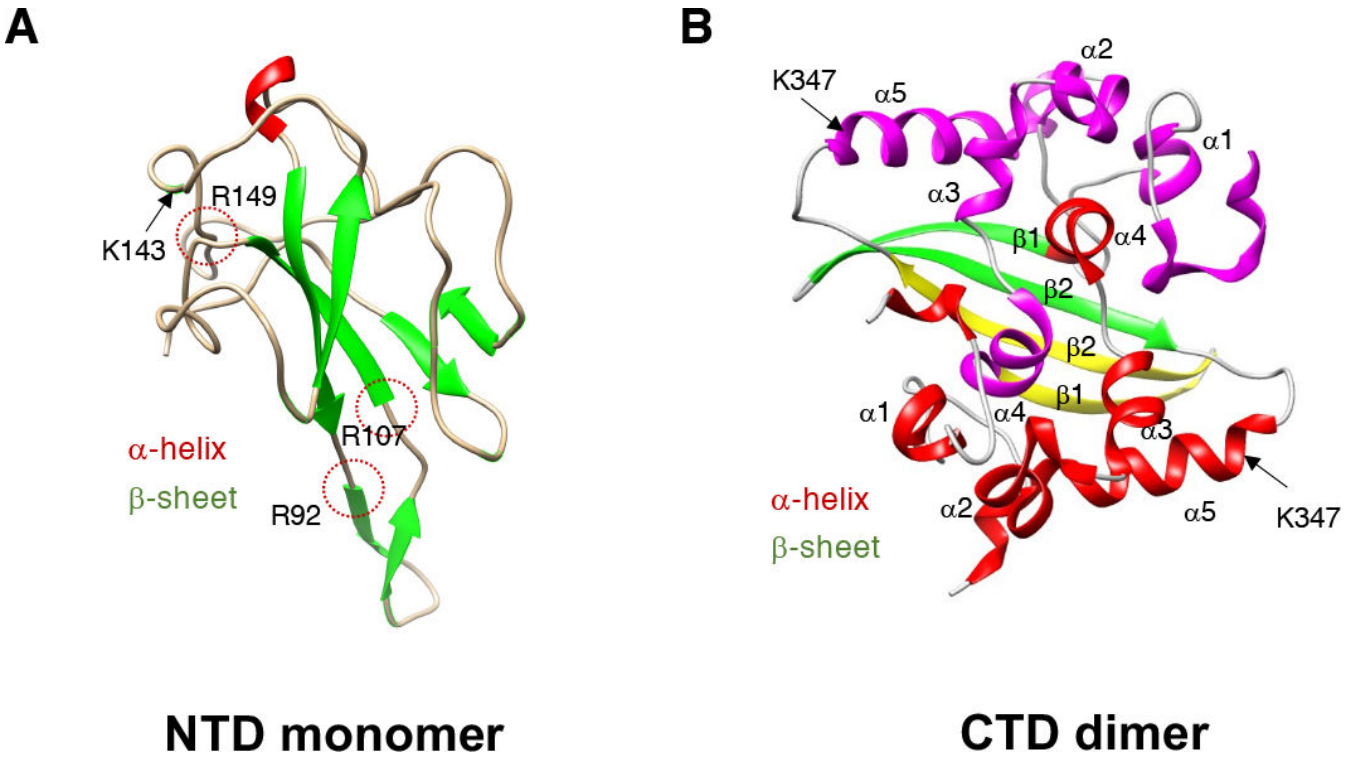

FIG 8 Structure of the SARS-CoV-2 NTD monomer and CTD dimer. (A and B) Ribbon view of the structure of the SARS-CoV-2 NTD monomer (A) (PDB accession code 7VNU) and CTD dimer (B) (PDB accession code 7C22). Location of residue K143 in the NTD and K347 in the CTD for ISGylation mapped onto the structure of the SARS-CoV-2 nucleocapsid of the NTD and CTD, respectively. Helices are shown in red (magenta) and strands in green (yellow). The images in panels (C and D) were prepared with the program UCSF Chimera (ChimeraX version 1.6).

oligomerization of WT nucleocapsid protein, but not K374R mutant, was suppressed by ISGylation (Fig. 13D, top panel, compare lane 2 with lane 4). These results suggest that ISGylation at K374 in the SB/N3 domain inhibits nucleocapsid oligomerization, thereby suppressing viral replication.

To exclude the possibility that ISGylation of the nucleocapsid protein inhibits the binding of the nucleocapsid protein to host mRNAs, we treated the cell lysates with or without RNase I during the cell harvesting process. Our results revealed that the treatment of the samples with RNase I efficiently degraded host mRNAs in HEK293T cells, as evidenced by a significant reduction in RNA concentration and reverse-transcribed-PCR signals of host mRNAs (Fig. 13E). Nuclear receptor interacting protein 1 (NRIP1) was examined as a target mRNA for SARS-CoV-2 nucleocapsid protein, and GAPDH served as a negative control. Under this experimental condition, treatment of the samples with RNase I did not affect nucleocapsid oligomerization (Fig. 13F, top panel, lanes 1 and 3). We observed the ISGylation-mediated suppression of nucleocapsid oligomerization after treatment of the sample with RNase I (Fig. 13F, top panel, lanes 2 and 4). These results indicate that the differences in the nucleocapsid signals are due to the disruption of nucleocapsid oligomerization, but not due to the differences in the amount of nucleocapsid-RNA complexes.

In conclusion, we propose a model in which the SARS-CoV-2 PLpro inhibits ISGylation of the nucleocapsid protein to promote viral replication by evading ISGylation-mediated disruption of the nucleocapsid oligomerization (Fig. 14).

DISCUSSION

IFN-inducible ISGylation has important roles in anti-viral activity against many types of RNA and DNA viruses (17). In the present study, we demonstrated that the SARS-CoV-2

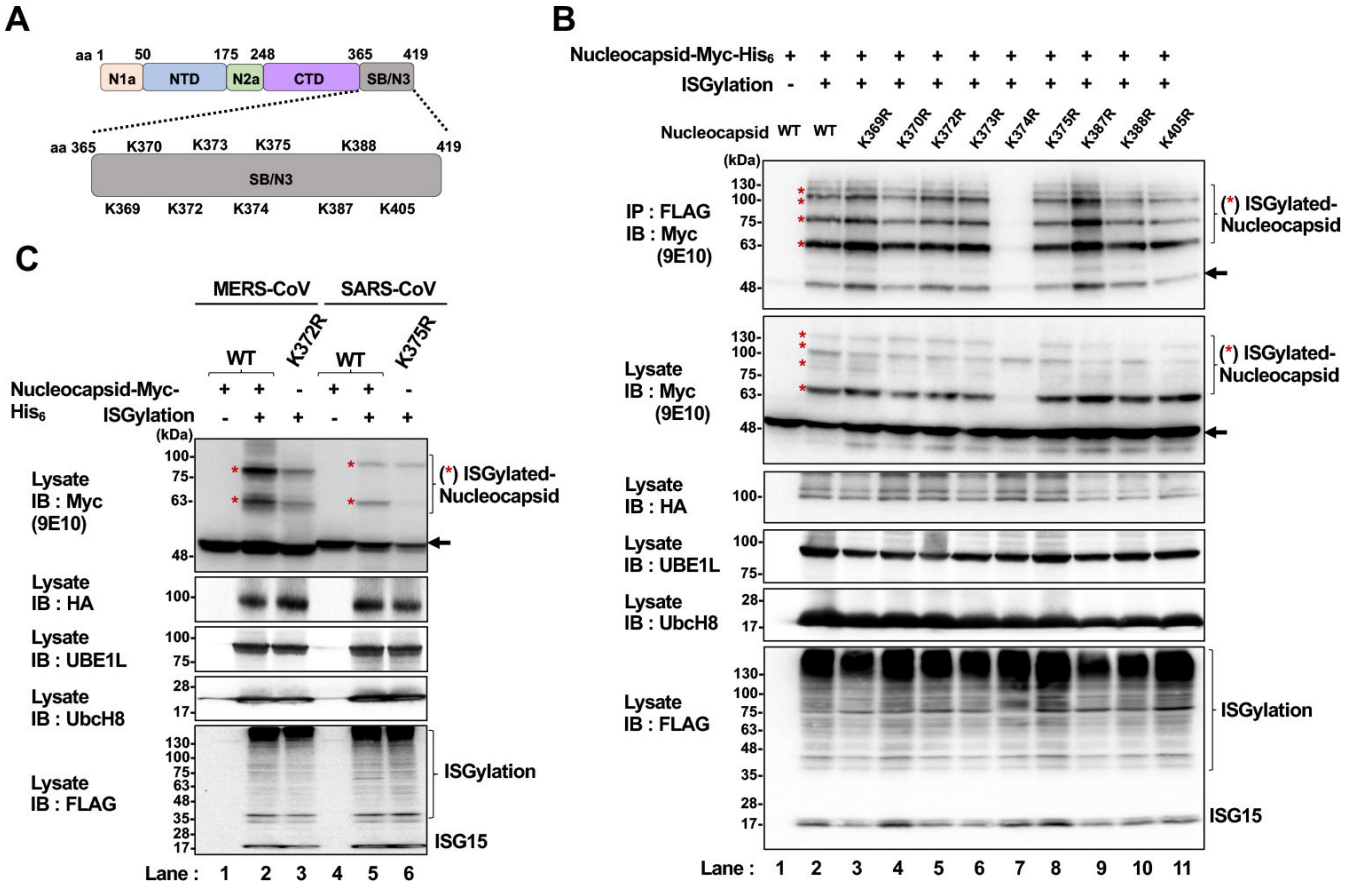

FIG 9 The residue K374 in the SB/N3 domain of SARS-CoV-2 nucleocapsid protein is a major acceptor lysine for ISGylation. (A) Schematic diagram of the SB/N3 domain of nucleocapsid from SARS-CoV-2 (WK-512). The nine lysine residues are located within the SB/N3 domain. (B) The expression plasmid encoding nucleocapsid-Myc-His_6 (pEF1-nucleocapsid-Myc-His_6) from SARS-CoV-2 (WK-512) or nucleocapsid Lys (K) mutants containing a point mutation of Lys to Arg at the corresponding Lys residues (K369R, K370R, K372R, K373R, K374R, K375R, K387R, K388R, or K405R) were co-expressed with pCAG-FLAG-ISG15 together with pCAG-UBE1L (E1), pCAG-UbcH8 (E2), and HA-tagged E3 ligase (pCAG-HA-HERC5) in 293T cells, followed by immunoprecipitation with anti-FLAG mouse mAb (M2) and detection with anti-Myc mouse mAb (9E10). (C) The expression plasmids encoding nucleocapsid WT-Myc-His_6 and nucleocapsid K372R-Myc-His_6 of MERS-CoV or nucleocapsid WT-Myc-His_6 and nucleocapsid K375R-Myc-His_6 of SARS-CoV were co-expressed with pCAG-FLAG-ISG15 together with pCAG-UBE1L (E1), pCAG-UbcH8 (E2), and pCAG-HA-HERC5 in 293T cells, followed by detection with anti-Myc mouse mAb (9E10). Input samples (indicated as lysate) were detected with anti-UBE1L rabbit mAb, anti-UbcH8 mouse mAb, anti-HA rabbit pAb, or anti-FLAG mouse mAb (M2) as indicated. Asterisk (*) indicates the ISG15-conjugated nucleocapsid proteins (ISGylated-nucleocapsid). The arrow indicates an authentic size of nucleocapsid-Myc-His_6. The immunoblots are representative of three independent experiments.

nucleocapsid protein is a target protein for ISGylation. We also found that HERC5 is a specific E3 ligase for nucleocapsid-ISGylation. Further mechanistic analysis revealed that nucleocapsid-ISGylation disrupts the nucleocapsid oligomerization, thereby inhibiting viral replication. Finally, we demonstrated that SARS-CoV-2 PLpro cleaves the ISG15 on the ISGylated nucleocapsid protein to evade ISGylation-mediated anti-viral activity. The present study is the first to show a regulatory role of ISGylation of SARS-CoV-2 nucleocapsid protein in the anti-viral activity against SARS-CoV-2 replication.

SARS-CoV-2 nucleocapsid protein is an RNA-binding protein and can bind to host mRNAs (24). Therefore, we performed experiments to exclude the possibility that ISGylation of the nucleocapsid protein inhibits the binding of the nucleocapsid protein to host mRNAs. Our results suggest that the differences in the nucleocapsid signals are due to the disruption of nucleocapsid oligomerization, but not due to the differences in the amount of nucleocapsid-RNA complexes (Fig. 13E and F).

SARS-CoV-2 nucleocapsid protein possesses domain structures, the NTD, which is responsible for RNA-binding, and the CTD, which is responsible for dimerization. The

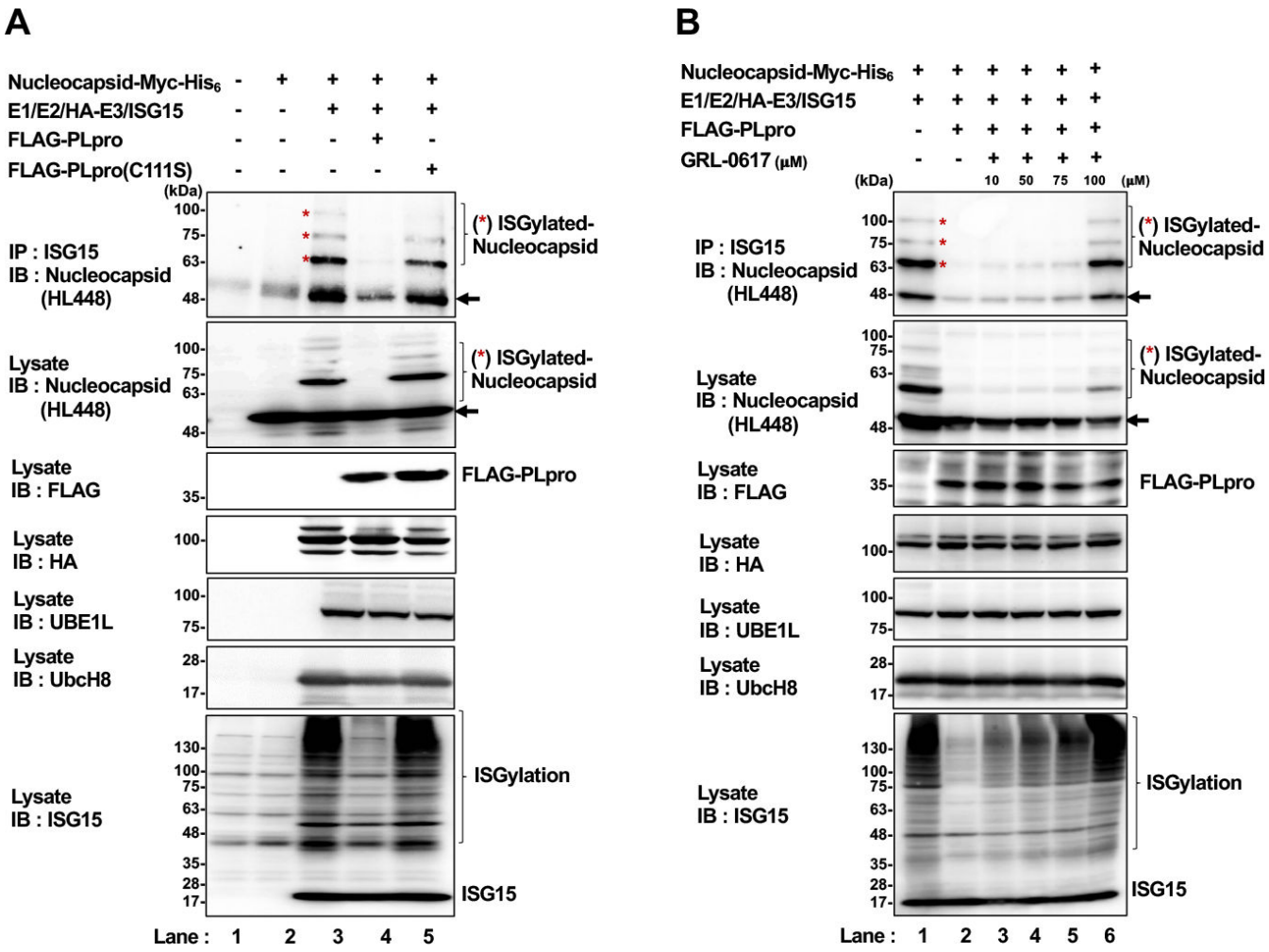

FIG 10 SARS-CoV-2 PLpro de-ISGylates the nucleocapsid protein. (A) The expression plasmid encoding nucleocapsid-Myc-His_6 from SARS-CoV-2 (WK-512), pEF1-nucleocapsid-Myc-His_6, was co-expressed with ISGylation machinery components, including pCAG- ISG15, pCAG-UBE1L (E1), pCAG-UbcH8 (E2), and pCAG-HA-HERC5 together with FLAG-tagged WT PLpro or the catalytically inactive mutant PLpro (C111S) in 293T cells, followed by immunoprecipitation with anti-ISG15 mouse mAb (F-9) and detection with anti-nucleocapsid rabbit mAb (HL448). (B) The expression plasmid encoding nucleocapsid-Myc-His_6 from SARS-CoV-2 (WK-512) was co-expressed with ISGylation machinery components, including pCAG-ISG15, E1, E2, and E3 ligase together with FLAG-tagged WT PLpro in 293T cells treated with dimethyl sulfoxide (DMSO) or GRL-0617, followed by immunoprecipitation with anti-ISG15 mouse mAb (F-9) and detection with anti-nucleocapsid rabbit mAb (HL448). Input samples (indicated as lysate) were detected with anti-nucleocapsid rabbit mAb (HL448), anti-UBE1L rabbit mAb, anti-UbcH8 mouse mAb, anti-HA rabbit pAb, anti-FLAG mouse mAb (M2), or anti-ISG15 mouse mAb (F-9) as indicated. Asterisk (*) indicates the ISG15-conjugated nucleocapsid proteins (ISGylated-nucleocapsid). The arrow indicates an authentic size of nucleocapsid-Myc-His_6. The immunoblots are representative of three independent experiments.

CTD-mediated dimer formation contributes to nucleocapsid oligomerization. Previous reports on SARS-CoV and human CoV (229E) had shown that the C-terminal SB/N3 region forms the higher-order assembly of tetramers and large oligomers (25). Recently, Ye and colleagues reported that the SB/N3 domain from SARS-CoV-2 possesses the putative short α-helices and forms a robust homo-tetramer through the association with the CTD dimers (9). Further investigation using higher-level reconstitution and/or high-resolution analysis is needed to understand the physiological and virological impacts of the SB/N3 domain. Here, we showed that the residue K374 in the SB/N3 domain is a major acceptor site for nucleocapsid-ISGylation, suggesting that the SB/N3 domain is a potential target for ISGylation-mediated anti-viral activity. Thus, we propose a mechanism in which ISGylation disrupts CTD-SB/N3-mediated nucleocapsid oligomerization to suppress viral

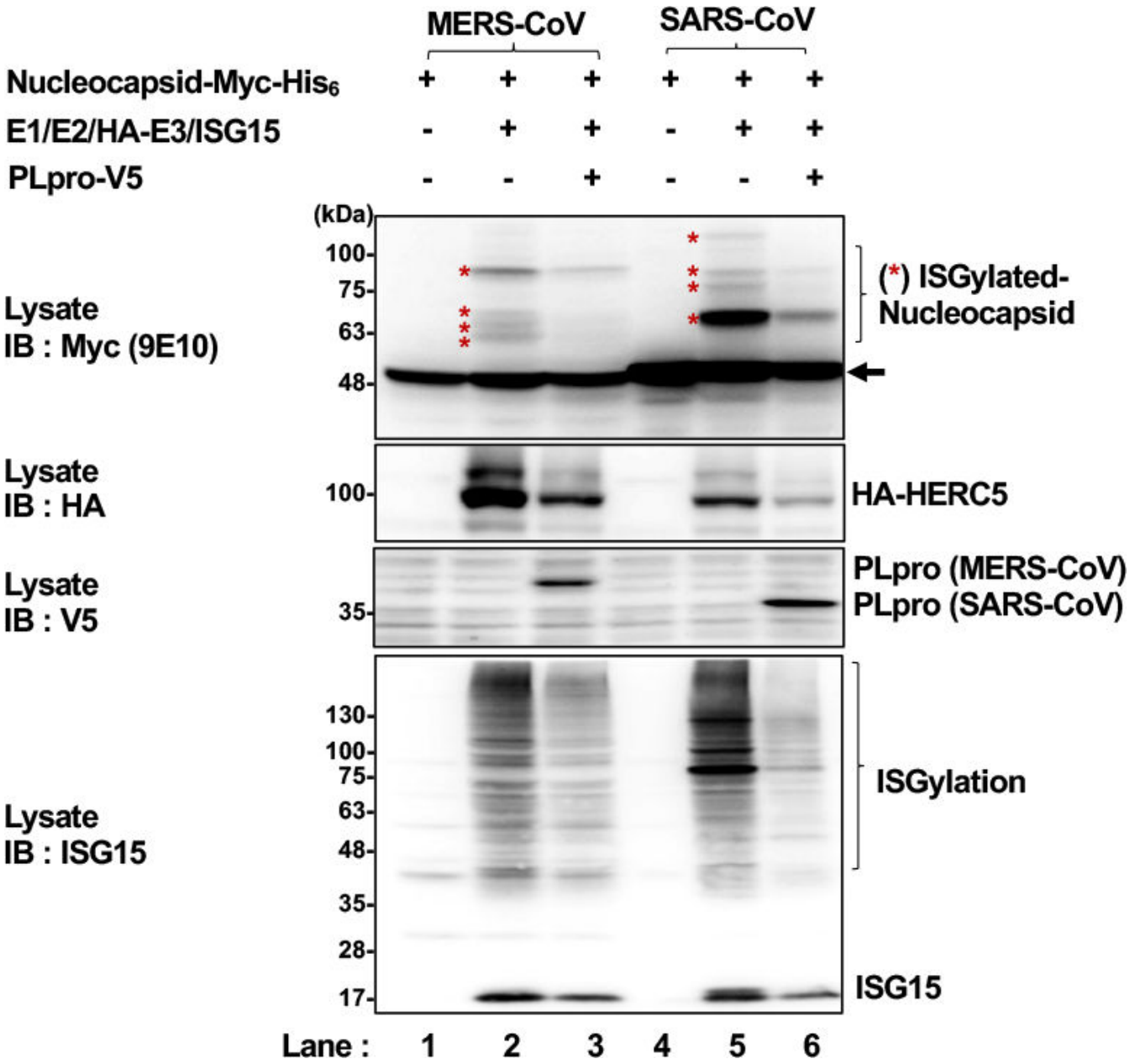

FIG 11 The viral protease (PLpro) from MERS-CoV and SARS-CoV inhibits ISGylation of the nucleocapsid protein. The expression plasmids encoding nucleocapsid-Myc-His_6 (pEF1-nucleocapsid-Myc-His_6) from SARS-CoV (WH20 strain) or MERS-CoV (EMC/2012 strain) were co-expressed with ISGylation components, including pCAG-FLAG-ISG15, pCAG-UBE1L (E1), pCAG-UbcH8 (E2), and HA-tagged E3 ligase (pCAG-HA-HERC5) together with their V5-tagged PLpro from SARS-CoV or MERS-CoV in 293T cells, followed by detection with anti-Myc mouse mAb (9E10). Input samples (indicated as lysate) were detected with anti-UBE1L rabbit mAb, anti-UbcH8 mouse mAb, anti-HA rabbit pAb, anti-V5 mouse mAb, or anti-ISG15 mouse mAb (F-9) as indicated. Asterisk (*) indicates the ISG15-conjugated nucleocapsid proteins (ISGylated-nucleocapsid). The arrow indicates an authentic size of nucleocapsid-Myc-His_6. The immunoblots are representative of three independent experiments.

replication (Fig. 14). The development of small molecules that can inhibit nucleocapsid oligomerization targeted to the CTD-SB/N3 domain merits further investigation.

We demonstrated that nucleocapsid-ISGylation exhibits slowly migrating forms of the nucleocapsid in the cells co-expressed with ISGylation machinery. Immunoblot analyses indicated that the mono-ISG15-conjugated form is approx. 63 kDa, which equals the molecular mass of one ISG15 (15 kDa) plus one nucleocapsid (48 kDa) (Fig. 2A through C, lane 3). On the other hand, the migrating form of approx. 75 kDa may be explained

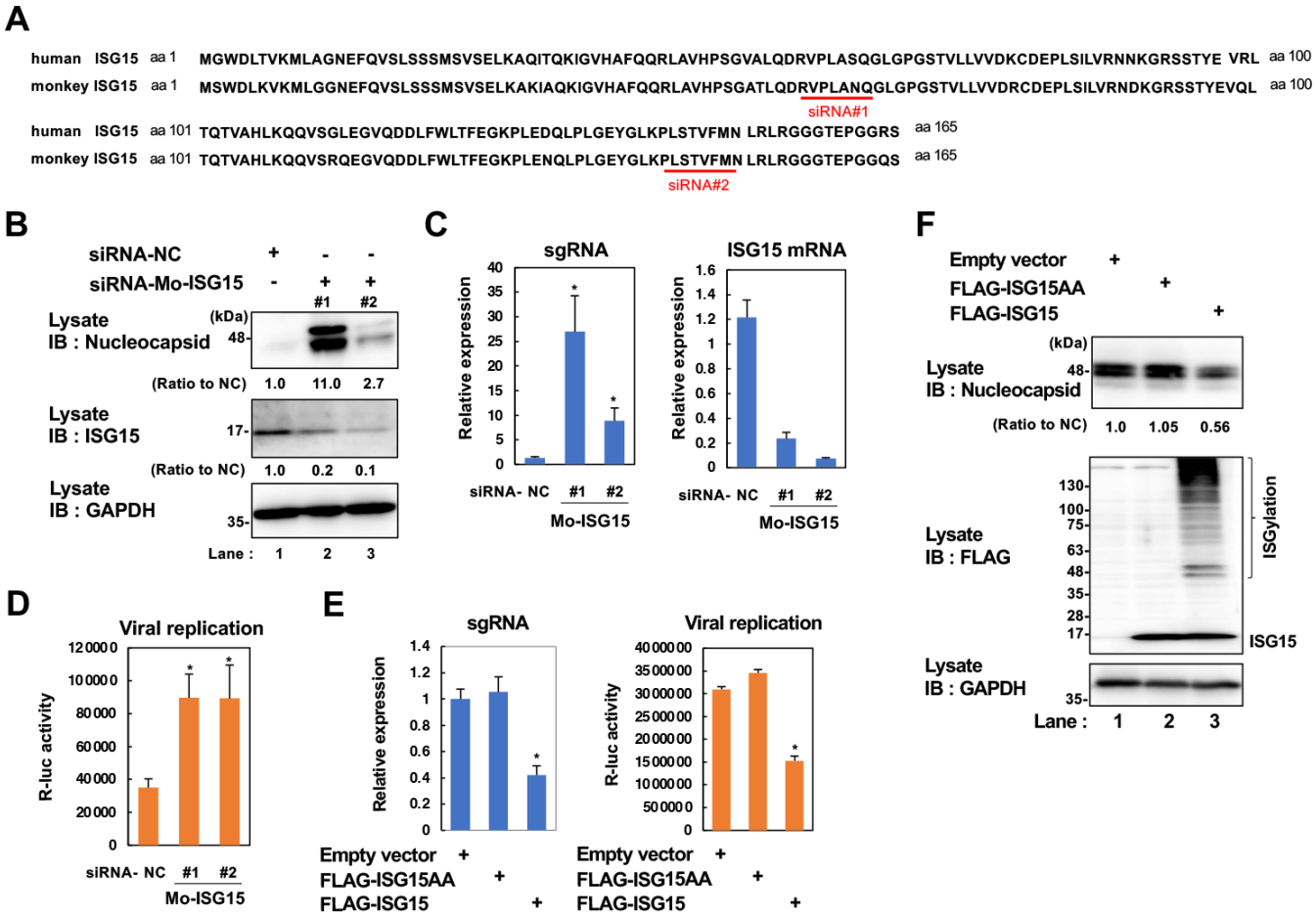

FIG 12 ISG15 functions as anti-viral activity in SARS-CoV-2 replication. (A) The amino acid sequence alignment of ISG15 from human and agm. Underlines indicate the target sites of siRNA to monkey ISG15 (siRNA#1 and siRNA#2). (B–D) SARS-CoV-2 reporter replicon cells (VeroE6/Rep3) were transfected with 50 nM of siRNA targeted to Mo-ISG15 (siRNA-Mo-ISG15#1, siRNA-Mo-ISG15#2) or negative control (NC) siRNA (siRNA-NC). After 72 h incubation, the cell lysates were harvested and subjected to immunoblotting with the indicated antibodies (B). The expression levels of sgRNA and ISG15 mRNA were determined by real-time PCR (C). The levels of viral RNA replication were measured by *Renilla* luciferase activity (D). (E and F) VeroE6/Rep3 cells were transfected with empty vector or plasmids expressing ISGylation components, including either pCAG-FLAG-ISG15 or pCAG-FLAG-ISG15-AA together with pCAG-UBE1L (E1), pCAG-UbcH8 (E2), and pCAG-HA-HERC5. After 72 h incubation, the levels of viral sgRNA expression and *Renilla* luciferase activity were measured by real-time PCR and luciferase assay (E). The cell lysates were subjected to immunoblotting with the indicated antibodies (F). Data from the real-time PCR were normalized to the amount of glyceraldehyde-3-phosphate dehydrogenase (GAPDH) mRNA expression. Results are the mean values of triplicates ± S.D. (n = 3 biological replicates). *P < 0.05 vs the results for the cells transfected with siRNA-NC (C and D) or the cells transfected with empty vector (E). The immunoblots are representative of three independent experiments.

as the result of a conjugation of di-ISG15 (Fig. 2A through C, lane 3). ISG15 is covalently conjugated to a target protein via a Lys residue as a monomer conjugation but not as a polymer conjugation (26). However, the migrating form of ISGylated nucleocapsid was also observed at around 100 kDa, suggesting that there might be a multi-ISGylated nucleocapsid protein via the residues of K143, K347, or K374. Another possibility is that an additional posttranslation modification, such as ubiquitin and ubiquitin-like modifiers (e.g., SUMOylation), is involved in nucleocapsid-ISGylation. This is supported by the report demonstrating that ubiquitin is a target of ISG15 conjugation in a protein degradation-independent manner (27). We had similar findings in our recent works on ISGylation of HCV NS5A protein and HBV HBx protein (22, 23). Further investigations are needed to clarify the possible poly-conjugation machinery of the ISGylated nucleocapsid proteins.

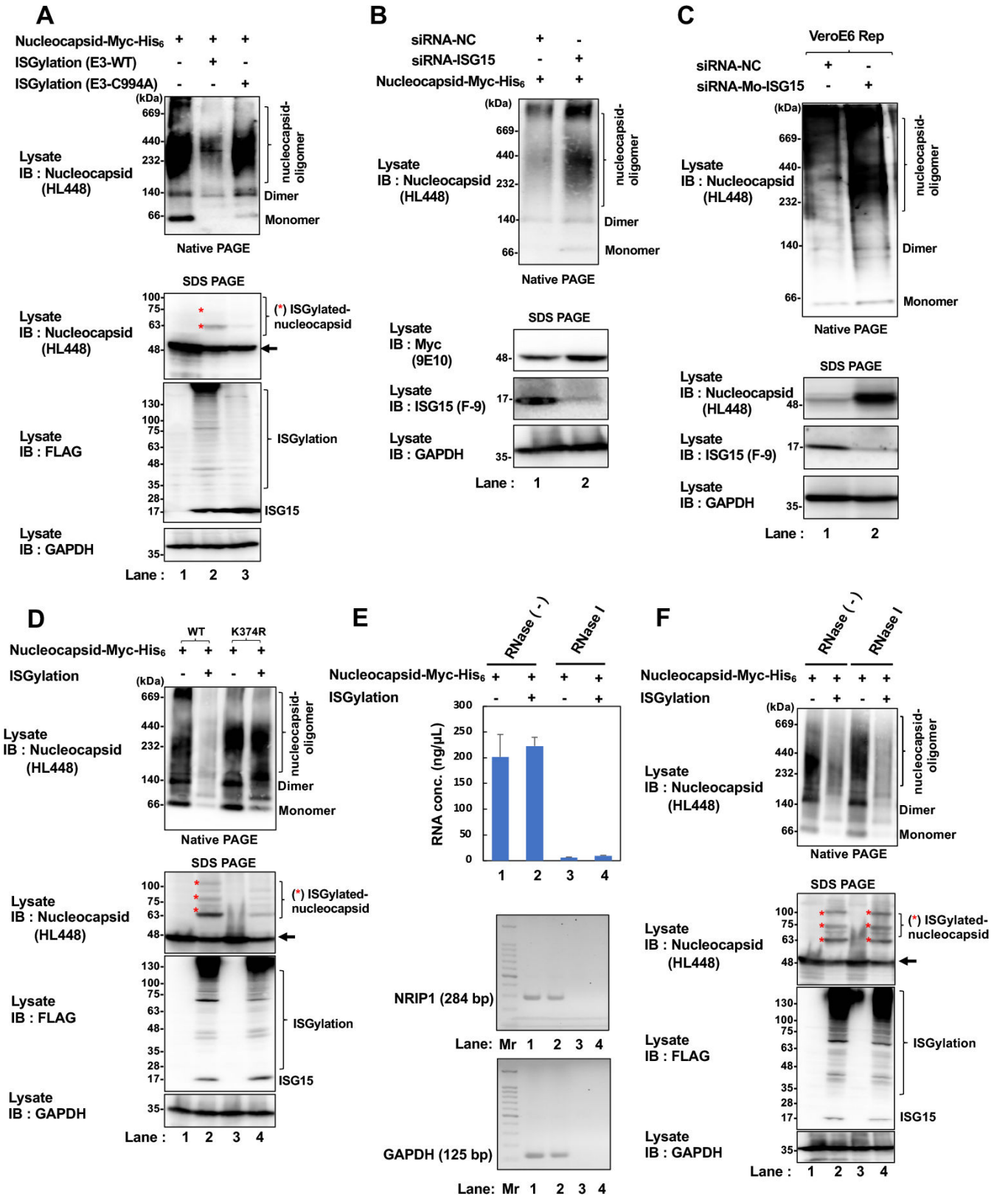

FIG 13 ISGylation inhibits SARS-CoV-2 replication through the disruption of viral nucleocapsid oligomerization. (A) The expression plasmid encoding nucleocapsid-Myc-His$_6$ from SARS-CoV-2 (WK-512) was co-transfected with pCAG-FLAG-ISG15 together with pCAG-UBE1L (E1), pCAG-UbcH8 (E2), and pCAG-HA-HERC5, or pCAG-HA-HERC5 C994A, in 293T cells. After 24 h of incubation, cells were harvested and applied to 3%–12% native-PAGE Novex Bis-Tris

(Continued on next page)

FIG 13 (Continued)

gel, followed by IB analysis with anti-nucleocapsid rabbit mAb (HL448). (B) HEK293T cells were transfected with 50 nM siRNA targeted to human ISG15 or NC siRNA (siRNA-NC). After 48 h of incubation, the cells were transfected with pEF1-nucleocapsid-Myc-His_6. After 24 h of incubation, cells were harvested. The samples were applied to 3%–12% native-PAGE Novex Bis-Tris gel, followed by IB analysis with anti-nucleocapsid rabbit mAb (HL448). (C) VeroE6/Rep3 cells were transfected with 50 nM siRNA targeted to Mo-ISG15 (siRNA-Mo-ISG15#1) or NC siRNA (siRNA-NC). After 72 h of incubation, cells were harvested. The samples were applied to 3%–12% native-PAGE Novex Bis-Tris gel, followed by IB analysis with anti-nucleocapsid rabbit mAb (HL448). Input samples were detected by sodium dodecyl sulfate (SDS)-PAGE analysis with nucleocapsid-specific antibody HL448 rabbit mAb or anti-FLAG mouse mAb as indicated. (D) The expression plasmid encoding either nucleocapsid-Myc-His_6 from SARS-CoV-2 (WT) or K374R mutant nucleocapsid-myc-His_6 was transfected into 293T cells together with pCAG-FLAG-ISG15, pCAG-UBE1L (E1), pCAG-UbcH8 (E2), and pCAG-HA-HERC5. After 24 h of incubation, cells were harvested. Cell lysates were applied to 3%–12% native-PAGE Novex Bis-Tris gel, followed by IB analysis with anti-nucleocapsid rabbit mAb (HL448). Input samples were detected by SDS-PAGE analysis with indicated antibodies. (E and F) The expression plasmid encoding nucleocapsid-Myc-His_6 was transfected together with pCAG-FLAG-ISG15, pCAG-UBE1L (E1), pCAG-UbcH8 (E2), and pCAG-HA-HERC5. After 24 h of incubation, cells were harvested. Cell lysates were treated with 0.1 U/µL RNase I prior to RNA extraction followed by gel electrophoresis (E) or native-PAGE and SDS-PAGE with indicated antibodies (F). Mr, DNA ladder markers. The asterisks (*) indicate ISGylated nucleocapsid. The arrow indicates an authentic size of nucleocapsid-Myc-His_6. The immunoblots are representative of three independent experiments.

To determine whether the nucleocapsid proteins produced from SARS-CoV-2 reporter replicon cells (VeroE6/Rep3) are ISGylated, the immunoblot analysis of the VeroE6/Rep3 cell lysates showed that ISGylated nucleocapsid proteins were hardly detected (Fig. 2D, third panel, lane 2). However, immunoprecipitation coupled with immunoblot analysis revealed that nucleocapsid proteins produced from the VeroE6/Rep3 cells were indeed ISGylated (Fig. 2D, top panel, lane 2). We speculated that the ISGylated nucleocapsid proteins were efficiently de-ISGylated by PLpro in the VeroE6/Rep3 cells, and the ISGylated nucleocapsid proteins were hardly detected with the straight Western blotting.

Additionally, we observed that residue K374 in the nucleocapsid protein from SARS-CoV-2 is responsible for the nucleocapsid-ISGylation, while the mutation of their conserved Lys (K) at SARS-CoV (K375) and MERS-CoV (K372) remained ISGylated nucleocapsid proteins (Fig. 9C), suggesting that other Lys (K) residues might be involved in nucleocapsid-ISGylation of SARS-CoV and MERS-CoV.

Viruses have evolved several counteracting strategies for achieving an immune escape from host defense machinery, including IFN-mediated anti-viral activity (28, 29). SARS-CoV-2 PLpro, which is a viral-encoded IFN antagonist, has been shown to cleave ISG15 conjugation and ubiquitin from target proteins. Recently, it was reported that SARS-CoV-2 PLpro preferentially cleaves ISG15 conjugation, whereas SARS-CoV PLpro predominantly cleaves ubiquitin chains (6, 7). Our results also showed that SARS-CoV-2 PLpro cleaves ISG15 conjugation on the ISGylated nucleocapsid protein more efficiently than those of SARS-CoV and MERS-CoV. These results suggest that SARS-CoV-2 has a greater capacity for escaping from the ISGylation-mediated anti-viral activity than SARS-CoV and MERS-CoV. Using GRL-0617, which is a selective inhibitor of SARS-CoV PLpro, we observed that GRL-0617 suppressed PLpro-mediated de-ISGylation activity on the ISGylated nucleocapsid protein (Fig. 10B). This result suggests that PLpro inhibitors may rescue the ISGylation-mediated anti-viral activity. The development of more potent and selective PLpro inhibitors against SARS-CoV-2 PLpro merits further investigation.

Liu and colleagues reported that the SARS-CoV-2 PLpro may inhibit the function of RNA sensor MDA5 rather than RIG-I through the ISG15-dependent activation and oligomerization of MDA5 (30). On the other hand, SARS-CoV-2 infection has been shown to promote the secretion of free ISG15, which in turn induces several pro-inflammatory cytokines in macrophage cells (31). Further study will be required to verify the roles of ISG15/ISGylation in the SARS-CoV-2 life cycle.

In summary, the present study demonstrated that the C-terminal SB/N3 domain on the SARS-CoV-2 nucleocapsid protein is a target for ISGylation-mediated anti-viral activity. Furthermore, SARS-CoV-2 PLpro preferentially cleaves ISG15 conjugation on the ISGylated nucleocapsid protein to escape from ISGylation-mediated anti-viral activity. Targeting the machinery of ISGylation to the SB/N3 domain of the nucleocapsid protein may lead to the development of more potent and selective inhibitors against SARS-CoV-2 infection.

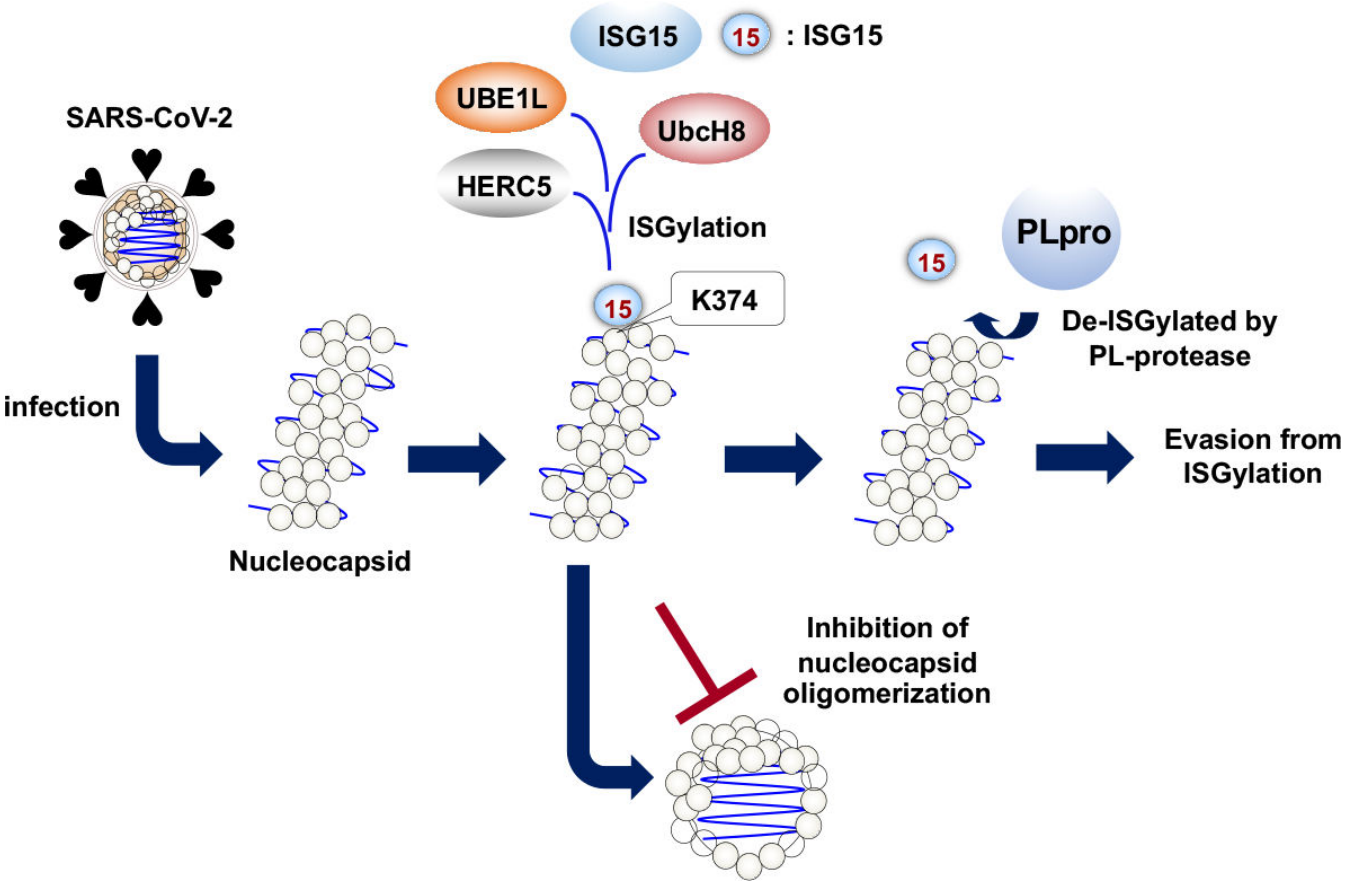

FIG 14 A proposed model. In the SARS-CoV-2 replicating cells, the viral nucleocapsid protein is targeted for ISGylation. The residue K374 in the C-terminal SB/N3 domain on the nucleocapsid protein is a major acceptor lysine for ISGylation. The ISGylated nucleocapsid protein results in interference with nucleocapsid oligomerization. The viral protease (PLpro) cleaves ISG15 on the ISGylated nucleocapsid protein to evade ISGylation-mediated anti-viral activity.

MATERIALS AND METHODS

Cell cultures

HEK293T cells were maintained in Dulbecco's modified Eagle's medium (DMEM) (high glucose) with L-glutamine (Fujifilm Wako Pure Chemical Industries, Osaka, Japan) supplemented with 50 IU/mL penicillin, 50 µg/mL streptomycin (Gibco, Grand Island, NY, USA), and 10% heat-inactivated fetal bovine serum (FBS) (Biowest, Nuaillé, France) at 37°C in a 5% CO_2 incubator. The SARS-CoV-2 replicon cells (VeroE6/Rep3) were reported previously (32). The VeroE6/Rep3 cells were cultured in DMEM supplemented with 50 IU/mL penicillin, 50 µg/mL streptomycin, 10% FBS, 1% sodium pyruvate (Sigma-Aldrich, St. Louis, MO, USA), and 1 mg/mL G418 (Nacalai Tesque, Japan). Cells were transfected with plasmid DNA using Trans IT reagents (Promega, Madison, WI, USA).

Plasmid construction

The full-length SARS-CoV-2 (WK-512 strain) genome was kindly provided by Prof. Y. Matsuura (Osaka University, Japan). The cDNA fragments encoding nucleocapsid (also referred to as ORF9) from SARS-CoV-2 were inserted into the EcoRI site of pEF1-Myc-His_6 (Invitrogen, Eugene, OR, USA) using an In-Fusion HD-Cloning kit (Clontech, Mountain View, CA, USA). Nucleocapsid Lys mutants containing mutations of Lys to Arg at the indicated Lys residues were generated by the mutagenesis PCR method using pEF1-nucleocapsid-Myc-His_6 as a template. The cDNA fragments encoding the nucleocapsids from NTD and N2a-CTD were amplified by PCR using pEF1-nucleocapsid-Myc-His_6 as

a template. The cDNA clones of the nucleocapsids from SARS-CoV (GenBank accession no. 828858.1) and MERS CoV (GenBank accession no. AFS88943.1) were purchased from Sino Biological (Kawasaki, Japan). The cDNA fragments encoding SARS-CoV-2 PLpro were amplified by PCR using a cDNA of nsp3 as a template and inserted into the XhoI and NotI sites of pCAG-FLAG (pCAG-FLAG-PLpro) using the In-Fusion HD-Cloning kit. The primer sequences used to construct SARS-CoV-2 expression plasmids used in this study are available from the authors upon request. The point mutant of PLpro (C111S) was generated by the mutagenesis PCR method using pCAG-FLAG-PLpro as a template as shown in Table 1. The cDNA fragments of PLpro derived from SARS-CoV (GenBank accession no. AY772062.1) and MERS-CoV (GenBank accession no. AFS88944) were cloned into the HindIII and XhoI sites of pSF-CMV-Puro-C-V5 (Invitrogen) using the In-Fusion HD-Cloning kit. The specific primers used for mutagenesis PCR and amplification PCR are described in Table 1 for oligonucleotides. All the PCR applications were conducted using Tks DNA Polymerase (TaKaRa Bio, Shiga, Japan). The expression plasmids for pCAG-UBE1L, pCAG-UbcH8, pCAG-HA-HERC5, pCAG-HA-HERC5(C994), pCAG-HA-TRIM25, pCAG-HA-HHARI, pCAG-FLAG-ISG15, and pCAG-FLAG-ISG15AA were previously described (22). The sequences of the inserts were extensively confirmed by sequencing (Eurofins Genomics, Tokyo, Japan).

Antibodies and reagents

The mouse mAbs used in this study were anti-c-Myc (9E10) mAb (Santa Cruz Biotechnology, Santa Cruz, CA, USA), anti-FLAG (M2) mAb (F-3165; Sigma-Aldrich, USA), anti-ISG15 (F-9) mAb (Santa Cruz Biotechnology, USA), anti-V5 mAb (ab27671; Abcam, Cambridge, UK), anti-Ube2L6 mAb (ab56502, Abcam, UK), anti-GFP mAb (ab184601; Abcam, UK), and anti-GAPDH mAb (MAB374; Millipore, Billerica, MA, USA).

The rabbit mAbs used in this study were anti-nucleocapsid-specific antibody (HL448) mAb (GTX635686; GeneTex, Inc., California, USA) and anti-Ube1L (EPR4270) mAb (ab108929; Abcam, UK). The rabbit pAb used in this study was anti-HA pAb (H-6908; Sigma-Aldrich, USA). Horseradish peroxidase (HRP)-conjugated anti-mouse IgG (Cell Signaling Technology, USA) and HRP-conjugated anti-rabbit IgG (Cell Signaling Technology, USA) were used as secondary antibodies. GRL0617 (SARS-CoV protease inhibitor) was purchased from Selleck Chemicals (Houston, TX, USA).

Immunoprecipitation and immunoblot analysis

Cells were transfected with the plasmids using Trans IT reagents (Promega), harvested at 48 h posttransfection, and suspended in 400 µL of radioimmunoprecipitation (RIPA) buffer containing 50 mM Tris-HCl (pH 8.0), 150 mM NaCl, 0.1% SDS, 1% NP-40, 0.5% deoxycholate, and protease inhibitor cocktail tablets (Roche Molecular Biochemicals, Mannheim, Germany). Cell lysates were incubated for 2 h at 4°C and centrifuged at 20,400 × *g* for 30 min at 4°C (Tomy centrifuge MX-307, Rotor Rack AR015-SC24; Tomy, Tokyo, Japan). The supernatant was incubated with appropriate antibodies at 4°C overnight and immunoprecipitated with protein G-Sepharose 4 Fast Flow (GE Healthcare, Buckinghamshire, UK).

After being washed with the lysis buffer five times, the samples were boiled in 15 µL of SDS sample buffer and then subjected to SDS-10% PAGE and transferred to polyvinylidene difluoride membranes (PVDF) (Millipore, USA). The membranes were blocked with Tris-buffered saline containing 20 mM Tris-HCl (pH 7.6), 135 mM NaCl, and 0.05% Tween 20 (TBST) containing 5% skim milk at room temperature for 2 h and incubated with the corresponding antibodies. The membranes were then incubated with HRP-conjugated secondary antibody at room temperature for 2 h. The immune complexes and cell lysates were visualized with ECL Western blotting detection reagents (GE Healthcare) and detected by an ImageQuant 800 system (GE Healthcare). The band intensities were quantified using ImageJ 1.53k software.

TABLE 1 Primers for PCR

Purpose	Name	Sequence (5′–3′)
PCR mutagenesis	pEF1-nucleocapsid(K38R)-Myc-His$_6$ forward	GGGGCGCGATCAAGACAACGTCGG
	pEF1-nucleocapsid(K38R)-Myc-His$_6$ reverse	CCGACGTTGTCTTGATCGCGCCCC
	pEF1-nucleocapsid(K61R)-Myc-His$_6$ forward	ACTCAACATGGCAGGGAAGACCTT
	pEF1-nucleocapsid(K61R)-Myc-His$_6$ reverse	AAGGTCTTCCCTGCCATGTTGAGT
	pEF1-nucleocapsid(K65R)-Myc-His$_6$ forward	AAGGAAGACCTTAGATTCCCTCGA
	pEF1-nucleocapsid(K65R)-Myc-His$_6$ reverse	TCGAGGGAATCTAAGGTCTTCCTT
	pEF1-nucleocapsid(K100R)-Myc-His$_6$ forward	GGTGGTGACGGTAGAATGAAAGAT
	pEF1-nucleocapsid(K100R)-Myc-His$_6$ reverse	ATCTTTCATTCTACCGTCACCACC
	pEF1-nucleocapsid(K102R)-Myc-His$_6$ forward	GACGGTAAAATGAGAGATCTCAGT
	pEF1-nucleocapsid(K102R)-Myc-His$_6$ reverse	ACTGAGATCTCTCATTTTACCGTC
	pEF1-nucleocapsid(K127R)-Myc-His$_6$ forward	TATGGTGCTAACAGAGACGGCATC
	pEF1-nucleocapsid(K127R)-Myc-His$_6$ reverse	GATGCCGTCTCTGTTAGCACCATA
	pEF1-nucleocapsid(K143R)-Myc-His$_6$ forward	TTGAATACACCAAGAGATCACATT
	pEF1-nucleocapsid(K143R)-Myc-His$_6$ reverse	AATGTGATCTCTTGGTGTATTCAA
	pEF1-nucleocapsid(K169R)-Myc-His$_6$ forward	ACAACATTGCCAAGAGGCTTCTAC
	pEF1-nucleocapsid(K169R)-Myc-His$_6$ reverse	GTAGAAGCCTCTTGGCAATGTTGT
	pEF1-nucleocapsid(K233/237R)-Myc-His$_6$ forward	CTTGAGAGCAGAATGTCTGGTAGA
	pEF1-nucleocapsid(K233/237R)-Myc-His$_6$ reverse	TCTACCAGACATTCTGCTCTCAAG
	pEF1-nucleocapsid(K248/249R)-Myc-His$_6$ forward	ACTGTCACTAGGAGATCTGCTGCT
	pEF1-nucleocapsid(K248/249R)-Myc-His$_6$ reverse	AGCAGCAGATCTCCTAGTGACAGT
	pEF1-nucleocapsid(K256/257R)-Myc-His$_6$ forward	GAGGCTTCTAGGAGGCCTCGGCAA
	pEF1-nucleocapsid(K256/257R)-Myc-His$_6$ reverse	TTGCCGAGGCCTCCTAGAAGCCTC
	pEF1-nucleocapsid(K261R)-Myc-His$_6$ forward	CCTCGGCAAAGACGTACTGCCACT
	pEF1-nucleocapsid(K261R)-Myc-His$_6$ reverse	AGTGGCAGTACGTCTTTGCCGAGG
	pEF1-nucleocapsid(K266R)-Myc-His$_6$ forward	ACTGCCACTAGAGCATACAATGTA
	pEF1-nucleocapsid(K266R)-Myc-His$_6$ reverse	TACATTGTATGCTCTAGTGGCAGT
	pEF1-nucleocapsid(K299R)-Myc-His$_6$ forward	ACTGATTACAGACATTGGCCGCAA
	pEF1-nucleocapsid(K299R)-Myc-His$_6$ reverse	TTGCGGCCAATGTCTGTAATCAGT
	pEF1-nucleocapsid(K338/342R)-Myc-His6 forward	GGTGCCATCAGATTGGATGACAGA
	pEF1-nucleocapsid(K338/342R)-Myc-His$_6$ reverse	TCTGTCATCCAATCTGATGGCACC
	pEF1-nucleocapsid(K347R)-Myc-His$_6$ forward	CCAAATTTCAGAGATCAAGTCATT
	pEF1-nucleocapsid(K347R)-Myc-His$_6$ reverse	AATGACTTGATCTCTGAAATTTGG
	pEF1-nucleocapsid(K355R)-Myc-His$_6$ forward	TTGCTGAATAGGCATATTGACGCA
	pEF1-nucleocapsid(K355R)-Myc-His$_6$ reverse	TGCGTCAATATGCCTATTCAGCAA
	pEF1-nucleocapsid(K361R)-Myc-His$_6$ forward	GACGCATACAGAACATTCCCACCA
	pEF1-nucleocapsid(K361R)-Myc-His$_6$ reverse	TGGTGGGAATGTTCTGTATGCGTC
	pEF1-nucleocapsid(K369R)-Myc-His$_6$ forward	CCAACAGAGCCTAGAAAGGACAAA
	pEF1-nucleocapsid(K369R)-Myc-His$_6$ reverse	TTTGTCCTTTCTAGGCTCTGTTGG
	pEF1-nucleocapsid(K370R)-Myc-His$_6$ forward	ACAGAGCCTAAAAGGACAAAAAG
	pEF1-nucleocapsid(K370R)-Myc-His$_6$ reverse	CTTTTTGTCCCTTTTAGGCTCTGT
	pEF1-nucleocapsid(K372R)-Myc-His$_6$ forward	CCTAAAAAGGACAGAAGAAGAAG
	pEF1-nucleocapsid(K372R)-Myc-His$_6$ reverse	CTTCTTCTTTCTGTCCTTTTTAGG
	pEF1-nucleocapsid(K373R)-Myc-His$_6$ forward	AAAAAGGACAAAAGGAAGAAGGCT
	pEF1-nucleocapsid(K373R)-Myc-His$_6$ reverse	AGCCTTCTTCCTTTTGTCCTTTT
	pEF1-nucleocapsid(K374R)-Myc-His$_6$ forward	AAGGACAAAAAGAGGAAGGCTGAT
	pEF1-nucleocapsid(K374R)-Myc-His$_6$ reverse	ATCAGCCTTCCTCTTTTTGTCCTT
	pEF1-nucleocapsid(K375R)-Myc-His$_6$ forward	GACAAAAAGAAGAGGGCTGATGAA
	pEF1-nucleocapsid(K375R)-Myc-His$_6$ reverse	TTCATCAGCCCTCTTCTTTTTGTC
	pEF1-nucleocapsid(K387R)-Myc-His$_6$ forward	CCGCAGAGACAGAGGAAACAGCAA
	pEF1-nucleocapsid(K387R)-Myc-His$_6$ reverse	TTGCTGTTTCCTCTGTCTCTGCGG
	pEF1-nucleocapsid(K388R)-Myc-His$_6$ forward	CCGCAGAGACAGAAGAGACAGCAA
	pEF1-nucleocapsid(K388R)-Myc-His$_6$ reverse	TTGCTGTCTCTTCTGTCTCTGCGG

(*Continued on next page*)

TABLE 1 Primers for PCR (*Continued*)

Purpose	Name	Sequence (5′–3′)
	pEF1-nucleocapsid(K405R)-Myc-His_6 forward	GATGATTTCTCCAGACAATTGCAA
	pEF1-nucleocapsid(K405R)-Myc-His_6 reverse	TTGCAATTGTCTGGAGAAATCATC
	Nucleocapsid(K372R)-MERS-CoV forward	CAGAAGGCTCCAAGGGAGGAGAGC
	Nucleocapsid(K372R)-MERS-CoV reverse	GCTCTCCTCCCTTGGAGCCTTCTG
	Nucleocapsid(K372R)-SARS-CoV forward	AAGGACAAGAAGAGGAAGACAGAT
	Nucleocapsid(K372R)-SARS-CoV reverse	ATCTGTCTTCCTCTTCTTGTCCTT
	pCAG-FLAG-PLpro(C111S) forward	GCAGATAACAACTCTTATCTTGCC
	pCAG-FLAG-PLpro(C111S) reverse	GGCAAGATAAGAGTTGTTATCTGC
PCR plasmid construction	pEF1-nucleocapsid-Myc-His_6 SARS-CoV-2 forward	TCCAGTGTGGTGGAAGGACCCCAAAATCAG
	pEF1-nucleocapsid-Myc-His_6 SARS-CoV-2 reverse	TGGATATCTGCAGAAGTCAGCACTGCTCAT
	pEF1-nucleocapsid-Myc-His_6 MERS-CoV forward	TCCAGTGTGGTGGAATTCATGGCAAGCCCTGCTGCCCCAAGGGCTGTG
	pEF1-nucleocapsid-Myc-His_6 MERS-CoV reverse	TGGATATCTGCAGAATTCATCTGTGTTCACATCAATCATAGGTCCAGG
	pEF1-nucleocapsid-Myc-His_6 SARS-CoV forward	TCCAGTGTGGTGGAATTCATGAGTGACAATGGACCACAGAGCAACCAG
	pEF1-nucleocapsid-Myc-His_6 SARS-CoV reverse	TGGATATCTGCAGAATTCAGCCTGGGTGCTGTCAGCAGAGGCTCCACT
	pEF1-nucleocapsid(NTD)-Myc-His_6 SARS-CoV-2 forward	TCCAGTGTGGTGGAATTCATGGCGTCTTGGTTCACCGCTCTCACT
	pEF1-nucleocapsid(NTD)-Myc-His_6 SARS-CoV-2 reverse	TGGATATCTGCAGAATTCCCCTTCTGCGTAGAAGCCTTTTGGCAA
	pEF1-nucleocapsid(N2a-CTD)-Myc-SARS-CoV-2 His_6 forward	TCCAGTGTGGTGGAATTCATGAGCAGAGGCGGCAGTCAAGCCTCT
	pEF1-nucleocapsid(N2a-CTD)-Myc-SARS-CoV-2 His_6 reverse	TGGATATCTGCAGAATTCTGGTGGGAATGTTTTGTATGCGTCAAT
	pCAG-FLAG-PLpro SARS-CoV-2 forward	ACGATAAAAACTCGAGCATGGAAGTGAGGACTATTAAGGTGTTT
	pCAG-FLAG-PLpro SARS-CoV-2 reverse	AGTGAATTCGCGGCCGCTCATTTTATGGTTGTTGTGTAACTGTT
	pSF-CMV-PLpro-V5 SARS-CoV forward	GCGGCCGCTGCCAAGCTTGCCACCATGGAGGTTAAGACTATAAAAGTG TTC
	pSF-CMV-PLpro-V5 SARS-CoV reverse	CGGTTTGCCGTACTCGAGATACGACACAGGCTTGATGGTTGTAGTGTA
	pSF-CMV-PLpro-V5 MERS-CoV forward	GCGGCCGCTGCCAAGCTTGCCACCATGTTAACAATCGAAGTCTTAGTGA CT
	pSF-CMV-PLpro-V5 MERS-CoV reverse	CGGTTTGCCGTACTCGAGTTGTCCATCAGACGATACAAGGCAGCTATT

Native-PAGE and Western blot analysis

Cells were harvested at 48 h of incubation and solubilized in the lysis buffer containing 150 mM NaCl, 50 mM Tris-HCl (pH 7.5), 1% NP-40, 1 mM EDTA, 10% glycerol, EDTA-free, and protease inhibitor cocktail (Roche). Cell lysates were incubated for 2 h at 4°C and centrifuged at 20,400 × *g* for 30 min at 4°C. To analyze the effect of nucleocapsid-RNA complexes on oligomerization, the lysis buffer was supplemented with or without 0.1 U/µL RNase I (RNase One Ribonuclease, M4261, Promega) and incubated for 30 min on ice, followed by centrifugation at 20,400 × *g* for 30 min at 4°C. The samples were prepared in NativePAGE sample buffers and then subjected to 3%–12% NativePAGE Novex Bis-Tris polyacrylamide gel electrophoresis (Invitrogen) and transferred to PVDF. The membranes were blocked with phosphate-buffered saline and 0.05% Tween 20 containing 5% skim milk at room temperature for 2 h and incubated with the corresponding antibodies. The membranes were then incubated with HRP-conjugated secondary antibody at room temperature for 2 h, visualized with ECL Western blotting detection reagents, and detected by an ImageQuant 800 system.

RNA interferences

siRNAs targeted to the agm ISG15 (siMo-ISG15 #1: 5′-GGGUUCCCCUUGCCAACCAdTdT-3′, siMo-ISG15 #2:

5′-UGAGCACCGUGUUCAUGAAdTdT-3′) were synthesized (Nippon Gene, Tokyo, Japan).

The siRNA targeted to the human ISG15 was previously described (22, 23). VeroE6/Rep3 cells were transfected with 50 nM siRNA using the RNAiMax transfection reagent (Life Technologies, Carlsbad, CA, USA) according to the manufacturer's instructions.

Real-time PCR

Total RNA was prepared using an RNeasy mini kit (Qiagen, Valencia, CA, USA), followed by cDNA synthesis using a GoScript reverse transcription system (Promega). The real-time PCR was performed using SYBR Premix Ex Taq II (Tli RNaseH Plus) (TaKaRa Bio, Shiga, Japan) according to the manufacturer's protocol. Fluorescent signals were analyzed by a StepOne Plus real-time PCR system (Applied Biosystems Inc., Foster City, CA, USA). The sgRNA, ISG15, and GAPDH genes were amplified using the specific primer pairs as follows: sgRNA sense primer, 5′-CGATCTCTTGTAGATCTGTTCTCT-3′; sgRNA antisense primer, 5′-GTCTTCCTTGCCATGTTGAGT-3′; ISG15 sense primer, 5′-AGCGAACTCATCTTTGC CAGTACA-3′; ISG15 antisense primer, 5′-CAGCTCTGACACCGACATGGA-3′; GAPDH sense primer, 5′-GCCATCAATGACCCCTTCATT-3′; GAPDH antisense primer, 5′-TCTCGCTCCTGGA AGATGG-3′.

The expression level of each gene was determined by the $\Delta\Delta C_T$ method using GAPDH as an internal control.

sgRNA sense primer, 5′-CGATCTCTTGTAGATCTGTTCTCT-3′.

Reverse-transcribed-PCR

Total RNA was prepared using an RNeasy mini kit (Qiagen, Valencia, CA, USA), followed by cDNA synthesis using a GoScript reverse transcription system (Promega). NRIP1 and GAPDH genes were amplified by PCR using the specific primer pairs as follows: NRIP1 sense primer, 5′-GCTGGGCATAATGAAGAGGA-3′; NRIP1 antisense primer, 5′-CAAAGAG GCCAGTAATGTGCTATC-3′; GAPDH sense primer, 5′-TCTCCTCTGACTTCAACAGCGACA-3′; GAPDH antisense primer, 5′-CCCTGTTGCTGTAGCCAAATTCGT-3′

The amplified PCR products were separated by 1.5% agarose gel electrophoresis.

Luciferase assay

Luciferase activity was measured using a *Renilla* luciferase assay system (Promega) according to the manufacturer's protocols. Cells were harvested at 72 h of incubation, solubilized in 1× passive lysis buffer according to the manufacturer's protocol, and measured using a Glomax Navigator Microplate Luminometer GM2000 (Promega).

Statistics

Results are expressed as the mean ± standard error. The comparison of the means of each group was performed using an independent *t*-test for Fig. 12C through E. *P*-values <0.05 were considered significant.

ACKNOWLEDGMENTS

We thank Y. Kozaki for the secretarial work.

This work was supported by the Kansai Economic Federation (I.S.). This work was also supported by the Ministry of Education, Culture, Sports, Science, and Technology (MEXT) of Japan, the Hyogo Science and Technology Association (T.A.), the Kobayashi Foundation (T.A.), the research grant by the President of Kobe Pharmaceutical University (I.S.), and the Nankai Building Service (I.S.). A.F.R. is supported by the MEXT scholarship, Global Leader Programs for ASEAN Sustainable Medical Development.

T.A. and I.S. conceived and designed the experiments. A.F.R. and T.A. carried out most of the experiments. H.K., C.M., L.D., Y.M., and F.S. assisted in the construction and the data analysis. T.T., C.O., K.M., and Y.M. contributed to the materials. T.A., A.F.R., and I.S. wrote the manuscript.

AUTHOR AFFILIATIONS

[1]Division of Infectious Disease Control, Center for Infectious Diseases, Kobe University Graduate School of Medicine, Kobe, Japan

[2]Faculty of Medicine, Public Health and Nursing, Universitas Gadjah Mada, Yogyakarta, Indonesia
[3]Department of Virology, Niigata University Graduate School of Medical and Dental Sciences, Niigata, Japan
[4]Department of Microbiology, Faculty of Medicine, Graduate Faculty of Interdisciplinary Research, University of Yamanashi, Yamanashi, Japan
[5]Division of Hepatitis Virology, Institute for Genetic Medicine, Hokkaido University, Hokkaido, Japan
[6]Center for Infectious Diseases Education and Research (CiDER), Osaka University, Osaka, Japan
[7]Drug Discovery Science, Division of Advanced Medical Science, Department of Science, Technology and Innovation, Graduate School of Science, Kobe University, Kobe, Japan
[8]Center for Cell Signaling and Medical Innovation, Kobe University Graduate School of Medicine, Kobe, Japan
[9]Laboratory of Virus Control, Research Institute for Microbial Diseases (RIMD), Osaka University, Osaka, Japan

AUTHOR ORCIDs

Kohji Moriishi http://orcid.org/0000-0002-9542-5188
Yoshiharu Matsuura http://orcid.org/0000-0001-9091-8285
Ikuo Shoji http://orcid.org/0000-0002-0730-4379

FUNDING

Funder	Grant(s)	Author(s)
Kansai Economic Federation (KEF)		Ikuo Shoji
Hyogo Science and Technology Association (HSTA)		Takayuki Abe
Ministry of Education, Culture, Sports, Science and Technology (MEXT)		Aulia Fitri Rhamadianti

AUTHOR CONTRIBUTIONS

Aulia Fitri Rhamadianti, Formal analysis, Investigation, Writing – original draft | Takayuki Abe, Conceptualization, Formal analysis, Funding acquisition, Investigation, Supervision, Writing – original draft, Writing – review and editing | Tomohisa Tanaka, Resources | Chikako Ono, Resources | Hisashi Katayama, Investigation | Yoshiteru Makino, Investigation | Lin Deng, Investigation | Chieko Matsui, Investigation | Kohji Moriishi, Resources | Fumi Shima, Investigation | Yoshiharu Matsuura, Resources | Ikuo Shoji, Conceptualization, Funding acquisition, Supervision, Writing – original draft, Writing – review and editing

DATA AVAILABILITY

The data that support the findings of this study are available at the Kernel-Kobe University Repository under ID 0100490883.

REFERENCES

1. Wu Z, McGoogan JM. 2020. Characteristics of and important lessons from the coronavirus disease 2019 (COVID-19) outbreak in China: summary of a report of 72 314 cases from the Chinese center for disease control and prevention. JAMA 323:1239–1242. https://doi.org/10.1001/jama.2020.2648
2. Trougakos IP, Terpos E, Alexopoulos H, Politou M, Paraskevis D, Scorilas A, Kastritis E, Andreakos E, Dimopoulos MA. 2022. Adverse effects of COVID-19 mRNA vaccines: the spike hypothesis. Trends Mol Med 28:542–554. https://doi.org/10.1016/j.molmed.2022.04.007
3. Esposito R, Mirra D, Sportiello L, Spaziano G, D'Agostino B. 2022. Overview of antiviral drug therapy for COVID-19: where do we stand? Biomedicines 10:2815. https://doi.org/10.3390/biomedicines10112815
4. Wang X, Sacramento CQ, Jockusch S, Chaves OA, Tao C, Fintelman-Rodrigues N, Chien M, Temerozo JR, Li X, Kumar S, Xie W, Patel DJ, Meyer C, Garzia A, Tuschl T, Bozza PT, Russo JJ, Souza TML, Ju J. 2022. Combination of antiviral drugs inhibits SARS-CoV-2 polymerase and exonuclease and demonstrates COVID-19 therapeutic potential in viral cell culture. Commun Biol 5:154. https://doi.org/10.1038/s42003-022-03101-9

5. Gordon DE, Jang GM, Bouhaddou M, Xu J, Obernier K, White KM, O'Meara MJ, Rezelj VV, Guo JZ, Swaney DL, et al. 2020. A SARS-CoV-2 protein interaction map reveals targets for drug repurposing. Nature 583:459–468. https://doi.org/10.1038/s41586-020-2286-9
6. Shin D, Mukherjee R, Grewe D, Bojkova D, Baek K, Bhattacharya A, Schulz L, Widera M, Mehdipour AR, Tascher G, Geurink PP, Wilhelm A, van der Heden van Noort GJ, Ovaa H, Müller S, Knobeloch K-P, Rajalingam K, Schulman BA, Cinatl J, Hummer G, Ciesek S, Dikic I. 2020. Papain-like protease regulates SARS-CoV-2 viral spread and innate immunity. Nature 587:657–662. https://doi.org/10.1038/s41586-020-2601-5
7. Klemm T, Ebert G, Calleja DJ, Allison CC, Richardson LW, Bernardini JP, Lu BG, Kuchel NW, Grohmann C, Shibata Y, et al. 2020. Mechanism and inhibition of the papain - like protease, PLpro, of SARS - CoV - 2. EMBO J 39:e106275. https://doi.org/10.15252/embj.2020106275
8. Lamers MM, Haagmans BL. 2022. SARS-CoV-2 pathogenesis. Nat Rev Microbiol 20:270–284. https://doi.org/10.1038/s41579-022-00713-0
9. Ye Q, West AMV, Silletti S, Corbett KD. 2020. Architecture and self - assembly of the SARS - CoV - 2 nucleocapsid protein. Protein Sci 29:1890–1901. https://doi.org/10.1002/pro.3909
10. Cubuk J, Alston JJ, Incicco JJ, Singh S, Stuchell-Brereton MD, Ward MD, Zimmerman MI, Vithani N, Griffith D, Wagoner JA, Bowman GR, Hall KB, Soranno A, Holehouse AS. 2021. The SARS-CoV-2 nucleocapsid protein is dynamic, disordered, and phase separates with RNA. Nat Commun 12:1936. https://doi.org/10.1038/s41467-021-21953-3
11. Jack A, Ferro LS, Trnka MJ, Wehri E, Nadgir A, Nguyenla X, Fox D, Costa K, Stanley S, Schaletzky J, Yildiz A. 2021. SARS-CoV-2 nucleocapsid protein forms condensates with viral genomic RNA. PLoS Biol 19:e3001425. https://doi.org/10.1371/journal.pbio.3001425
12. Ribeiro-Filho HV, Jara GE, Batista FAH, Schleder GR, Costa Tonoli CC, Soprano AS, Guimarães SL, Borges AC, Cassago A, Bajgelman MC, Marques RE, Trivella DBB, Franchini KG, Figueira ACM, Benedetti CE, Lopes-de-Oliveira PS. 2022. Structural dynamics of SARS-CoV-2 nucleocapsid protein induced by RNA binding. PLoS Comput Biol 18:e1010121. https://doi.org/10.1371/journal.pcbi.1010121
13. Yan W, Zheng Y, Zeng X, He B, Cheng W. 2022. Structural biology of SARS-CoV-2: open the door for novel therapies. Signal Transduct Target Ther 7:26. https://doi.org/10.1038/s41392-022-00884-5
14. Mu J, Fang Y, Yang Q, Shu T, Wang A, Huang M, Jin L, Deng F, Qiu Y, Zhou X. 2020. SARS-CoV-2 N protein antagonizes type I interferon signaling by suppressing phosphorylation and nuclear translocation of STAT1 and STAT2. Cell Discov 6:65. https://doi.org/10.1038/s41421-020-00208-3
15. Zheng Z-Q, Wang S-Y, Xu Z-S, Fu Y-Z, Wang Y-Y. 2021. SARS-CoV-2 nucleocapsid protein impairs stress granule formation to promote viral replication. Cell Discov 7:38. https://doi.org/10.1038/s41421-021-00275-0
16. Liu H, Bai Y, Zhang X, Gao T, Liu Y, Li E, Wang X, Cao Z, Zhu L, Dong Q, Hu Y, Wang G, Song C, Niu X, Zheng T, Wang D, Liu Z, Jin Y, Li P, Bian X, Cao C, Liu X. 2022. SARS-CoV-2 N protein antagonizes stress granule assembly and IFN production by interacting with G3BPs to facilitate viral replication. J Virol 96:e0041222. https://doi.org/10.1128/jvi.00412-22
17. Dzimianski JV, Scholte FEM, Bergeron É, Pegan SD. 2019. ISG15: it's complicated. J Mol Biol 431:4203–4216. https://doi.org/10.1016/j.jmb.2019.03.013
18. Zhang D, Zhang D-E. 2011. Interferon-stimulated gene 15 and the protein ISGylation system. J Interferon Cytokine Res 31:119–130. https://doi.org/10.1089/jir.2010.0110
19. Malakhov MP, Malakhova OA, Kim KI, Ritchie KJ, Zhang D-E. 2002. UBP43 (USP18) specifically removes ISG15 from conjugated proteins. J Biol Chem 277:9976–9981. https://doi.org/10.1074/jbc.M109078200
20. Isaacson MK, Ploegh HL. 2009. Ubiquitination, ubiquitin-like modifiers, and deubiquitination in viral infection. Cell Host Microbe 5:559–570. https://doi.org/10.1016/j.chom.2009.05.012
21. Perng Y-C, Lenschow DJ. 2018. ISG15 in antiviral immunity and beyond. Nat Rev Microbiol 16:423–439. https://doi.org/10.1038/s41579-018-0020-5
22. Abe T, Minami N, Bawono RG, Matsui C, Deng L, Fukuhara T, Matsuura Y, Shoji I. 2020. ISGylation of hepatitis C virus NS5A protein promotes viral RNA replication via recruitment of cyclophilin A. J Virol 94:e00532-20. https://doi.org/10.1128/JVI.00532-20
23. Bawono RG, Abe T, Qu M, Kuroki D, Deng L, Matsui C, Ryo A, Suzuki T, Matsuura Y, Sugiyama M, Mizokami M, Shimotohno K, Shoji I. 2021. HERC5 E3 ligase mediates ISGylation of hepatitis B virus X protein to promote viral replication. J Gen Virol 102. https://doi.org/10.1099/jgv.0.001668
24. Nabeel-Shah S, Lee H, Ahmed N, Burke GL, Farhangmehr S, Ashraf K, Pu S, Braunschweig U, Zhong G, Wei H, Tang H, Yang J, Marcon E, Blencowe BJ, Zhang Z, Greenblatt JF. 2022. SARS-CoV-2 nucleocapsid protein binds host mRNAs and attenuates stress granules to impair host stress response. iScience 25:103562. https://doi.org/10.1016/j.isci.2021.103562
25. Lo Y-S, Lin S-Y, Wang S-M, Wang C-T, Chiu Y-L, Huang T-H, Hou M-H. 2013. Oligomerization of the carboxyl terminal domain of the human coronavirus 229E nucleocapsid protein. FEBS Lett 587:120–127. https://doi.org/10.1016/j.febslet.2012.11.016
26. Okumura F, Okumura AJ, Uematsu K, Hatakeyama S, Zhang D-E, Kamura T. 2013. Activation of double-stranded RNA-activated protein kinase (PKR) by interferon-stimulated gene 15 (ISG15) modification down-regulates protein translation. J Biol Chem 288:2839–2847. https://doi.org/10.1074/jbc.M112.401851
27. Fan J-B, Arimoto K, Motamedchaboki K, Yan M, Wolf DA, Zhang D-E. 2015. Identification and characterization of a novel ISG15-ubiquitin mixed chain and its role in regulating protein homeostasis. Sci Rep 5:12704. https://doi.org/10.1038/srep12704
28. Chan YK, Gack MU. 2016. Viral evasion of intracellular DNA and RNA sensing. Nat Rev Microbiol 14:360–373. https://doi.org/10.1038/nrmicro.2016.45
29. Abe T, Shapira SD. 2019. Negative regulation of cytosolic sensing of DNA, p 91–115. In International review of cell and molecular biology. Elsevier.
30. Liu G, Lee J-H, Parker ZM, Acharya D, Chiang JJ, van Gent M, Riedl W, Davis-Gardner ME, Wies E, Chiang C, Gack MU. 2021. ISG15-dependent activation of the sensor MDA5 is antagonized by the SARS-CoV-2 papain-like protease to evade host innate immunity. Nat Microbiol 6:467–478. https://doi.org/10.1038/s41564-021-00884-1
31. Munnur D, Teo Q, Eggermont D, Lee HHY, Thery F, Ho J, van Leur SW, Ng WWS, Siu LYL, Beling A, Ploegh H, Pinto-Fernandez A, Damianou A, Kessler B, Impens F, Mok CKP, Sanyal S. 2021. Altered ISGylation drives aberrant macrophage-dependent immune responses during SARS-CoV-2 infection. Nat Immunol 22:1416–1427. https://doi.org/10.1038/s41590-021-01035-8
32. Tanaka T, Saito A, Suzuki T, Miyamoto Y, Takayama K, Okamoto T, Moriishi K. 2022. Establishment of a stable SARS-CoV-2 replicon system for application in high-throughput screening. Antiviral Res 199:105268. https://doi.org/10.1016/j.antiviral.2022.105268